

# Magnetic White Dwarf Stars in the Sloan Digital Sky Survey

S. O. Kepler<sup>1\*</sup>, I. Pelisoli<sup>1</sup>, S. Jordan<sup>2</sup>, S. J. Kleinman<sup>3</sup>,  
 D. Koester<sup>4</sup>, B. Külebi<sup>5,6</sup>, V. Peçanha<sup>1</sup>, B. G. Castanheira<sup>7,8</sup>, A. Nitta<sup>3</sup>,  
 J.E.S. Costa<sup>1</sup>, D. E. Winget<sup>8</sup>, A. Kanaan<sup>9</sup>, and L. Fraga<sup>10</sup>

<sup>1</sup>*Instituto de Física, Universidade Federal do Rio Grande do Sul, 91501-900 Porto-Alegre, RS, Brazil*

<sup>2</sup>*Astronomisches Rechen-Institut, Zentrum für Astronomie der Universität Heidelberg, Mönchhofstr. 12-14, D-69120 Heidelberg, Germany*

<sup>3</sup>*Gemini Observatory, Hilo, Hawaii, 96720, USA*

<sup>4</sup>*Institut für Theoretische Physik und Astrophysik, Universität Kiel, 24098 Kiel, Germany*

<sup>5</sup>*Institut de Ciències de l’Espai, Universitat Autònoma de Barcelona, Barcelona, Spain*

<sup>6</sup>*Institute for Space Studies of Catalonia, c/Gran Capità 2-4, Edif. Nexus 104, 08034 Barcelona, Spain*

<sup>7</sup>*Institut für Astronomie, Wien, Austria*

<sup>8</sup>*McDonald Observatory and Department of Astronomy, University of Texas, Austin, TX, 78712, USA*

<sup>9</sup>*Universidade Federal de Santa Catarina, Florianópolis, SC, Brazil*

<sup>10</sup>*Soar Telescope, La Serena, Chile*

Accepted Received

## ABSTRACT

To obtain better statistics on the occurrence of magnetism among white dwarfs, we searched the spectra of the hydrogen atmosphere white dwarf stars (DAs) in the Data Release 7 of the Sloan Digital Sky Survey (SDSS) for Zeeman splittings and estimated the magnetic fields. We found 521 DAs with detectable Zeeman splittings, with fields in the range from around 1 MG to 733 MG, which amounts to 4% of all DAs observed. As the SDSS spectra has low signal-to-noise ratios, we carefully investigated by simulations with theoretical spectra how reliable our detection of magnetic field was.

**Key words:** stars: – white dwarfs – magnetic field

## 1 INTRODUCTION

In the latest white dwarf catalog based on the Sloan Digital Sky Survey (SDSS) Data Release 7 (DR7), Kleinman et al. (2013) classify the spectra of 19 713 white dwarf stars, including 12 831 hydrogen atmosphere white dwarf stars (DAs) and 922 helium atmosphere white dwarf stars (DBs). The authors fit the optical spectra from 3 900Å to 6 800Å to DA and DB grids of synthetic non-magnetic spectra derived from model atmospheres (Koester 2010). The SDSS spectra have a mean g-band signal-to-noise ratio  $S/N(g) \approx 13$  for all DAs, and  $S/N(g) \approx 21$  for those brighter than  $g=19$ .

Through visual inspection of all these spectra, we identified Zeeman splittings in the spectra of 521 DA white dwarfs, eleven with multiple spectra. The main object of this paper is to identify these stars and estimate their magnetic field. Independently, Külebi et al. (2009) found 44 new magnetic white dwarfs in the same SDSS DR7 sample, and used  $\log g = 8.0$  models to estimate the fields of the 141 then known magnetic white dwarfs, finding fields from  $B=1$  MG to 733 MG. We report here on the estimate of the Zeeman splittings in  $\simeq 4\%$  of all DA white dwarf stars. With the low resolution ( $R \simeq 2000$ ) of the SDSS spectra, magnetic fields weaker than 2 MG are only detectable for the highest S/N spectra (e.g. Tout et al. 2008). We first summarize some previous results on magnetic white dwarfs.

\* kepler@if.ufrgs.br

## 2 MAGNETIC WHITE DWARFS AND THEIR PROGENITORS

The magnetic nature of the until then unexplained spectra of the white dwarf GRW+70.8247 was confirmed by Kemp (1970). His magneto-emission model, which predicted the level of continuum polarization, was not quite adequate for the high magnetic field in this star, and the estimated field strength of 10 MG later turned out to be much too low, but the general idea that the strange spectrum was caused by a magnetic field was correct. The detailed description of the spectra became possible only with extensive calculations of the atomic transitions of hydrogen developed by Roesner et al. (1984) and Greenstein, Henry, & O'Connell (1985), and a consistent atmospheric modeling by Wickramasinghe & Ferrario (1988) and Jordan (1992).

The numbers of known magnetic white dwarfs has increased significantly since the first identifications. Liebert, Bergeron, & Holberg (2003) found that only 2% of the 341 DAs and 15 DBs in the Palomar-Green Survey (PG) were magnetic, i.e., exhibited Zeeman splitted lines. However, they estimated that up to 10% could be magnetic, if the magnetic white dwarfs are more massive than average white dwarfs and therefore had smaller radius and luminosities, as indicated by Liebert et al. (1988) and Sion et al. (1988). Kawka et al. (2003) estimated up to 16% of all white dwarfs may be magnetic. Jordan et. al. (2007), based on spectropolarimetry using the 8.2 m telescope VLT at ESO estimate up to 15 to 20% of all white dwarfs are magnetic at the kG level. Landstreet et al. (2012) reanalyzed the spectropolarimetry with a new state-of-the-art calibration pipeline and added further new observations. From the total sample of 35 DA stars they found that about 10% (between 2.8% and 30% at the 95% confidence level) were magnetic on the kG level.

An accurate estimate of this percentage is crucial for an understanding of the origin of the magnetic fields. In the local 20 and 25 pc volume limited sample, there are  $\simeq 7\%$  magnetic white dwarfs, according to Giammiceli, Bergeron, & Dufour (2012) and Holberg, Sion, & Oswalt (2011).

Historically, the explanation of the magnetic fields in white dwarfs has been as fossil fields, motivated by the slow Ohmic decay in degenerate matter (e.g. Braithwaite & Spruit 2004; Tout, Wickramasinghe, & Ferrario 2004; Wickramasinghe & Ferrario 2005). From the discovery of kilo Gauss (kG) magnetic fields in the atmospheres of peculiar early type stars, the Ap and Bp stars, already Babcock (1947,a) demonstrated that conservation of the magnetic flux during the stellar evolution could lead to field strengths as high as a million Gauss (MG) in the white dwarfs resulting from the evolution.

Ap/Bp stars constitute less than 10% of all intermediate mass main sequence stars (e.g. Power et al. 2008), and can account for a fraction of 4.3% magnetic white dwarfs, but they should produce white dwarfs with fields above 100 MG (Kawka et al. 2003) if magnetic flux is fully conserved during stellar evolution. Wickramasinghe & Ferrario (2005), via population synthesis, conclude that the current number distribution and masses of high-field magnetic white dwarfs (HFMWDs,  $B > 1$  MG) can be explained if  $\approx 40\%$  of main-sequence stars more massive than  $4.5 M_{\odot}$  have magnetic fields in the range of 10-100 G, which is below the current level of detection.

Schmidt & Smith (1995); Liebert et al. (1988); Sion et al. (1988); Liebert, Bergeron, & Holberg (2003) and Kawka et al. (2007) find that magnetic white dwarfs are more massive than non-magnetic ones by fitting the wings of the spectral lines to theoretical spectra, supposedly unaffected by the magnetic fields. Tout & Regos (1995); Tout et al. (2008) and Nordhaus (2011) propose white dwarfs with fields above 1 MG are produced by strong binary interactions during post-main sequence evolution, while García-Berro et al. (2012) proposes that high magnetic field white dwarfs are produced by the merger of two degenerate cores and that the expected number agrees with observations. These proposals are in line with the cited observation that magnetic white dwarf stars have, in general, higher masses than average single white dwarf stars. Kundu & Mukhopadhyay (2012) and Das & Mukhopadhyay (2012) propose highly magnetic white dwarfs could have limiting masses substantially higher than the Chandrasekhar limit. On the other hand, Wegg & Phinney (2012) conclude that the kinematics of massive white dwarfs are consistent with the majority being formed from single star evolution.

## 3 DETECTION OF MAGNETIC FIELD IN SDSS DR7 WDS

We classified more than 48 000 spectra, selected as possible white dwarf stars from the Sloan Digital Sky Survey Data Release 7 by their colors, through visual inspection and detected Zeeman splittings in 521 DA stars. Figure 1 shows the spectra of one of the newly identified magnetic white dwarfs as an example. As we were only able to detect magnetic fields down to 1–3 MG in strength, because of the  $R \simeq 2000$  resolution and relatively low signal-to-noise of most spectra ( $\langle S/N \rangle \simeq 13$ ), the 4% detected (521/12831 DAs) is a lower limit and the actual number of magnetic white dwarf stars should be larger if we include smaller field strengths. The identified magnetic white dwarf stars cover the whole range of temperature and spectral classes observed (Kleinman et al. 2013). Figures 2 and 3 show spectra of a few of the highest S/N new magnetic white dwarfs we identified, showing a broad range of splittings, and hence of magnetic fields.

Fig. 4 shows the fraction of detected magnetism in white dwarfs as a function of the signal-to-noise (S/N) ratio provided by Kleinman et al. (2013). The fact that we see an increase of detected magnetic fields in spectra with lower S/N ratios made us suspicious. For this reason we carefully investigated the influence of the S/N ratio on the detection rate with the help of a blind test using noisy theoretical spectra (see Sect. 4). Our result was that classification with  $S/N \leq 10$  need to be confirmed

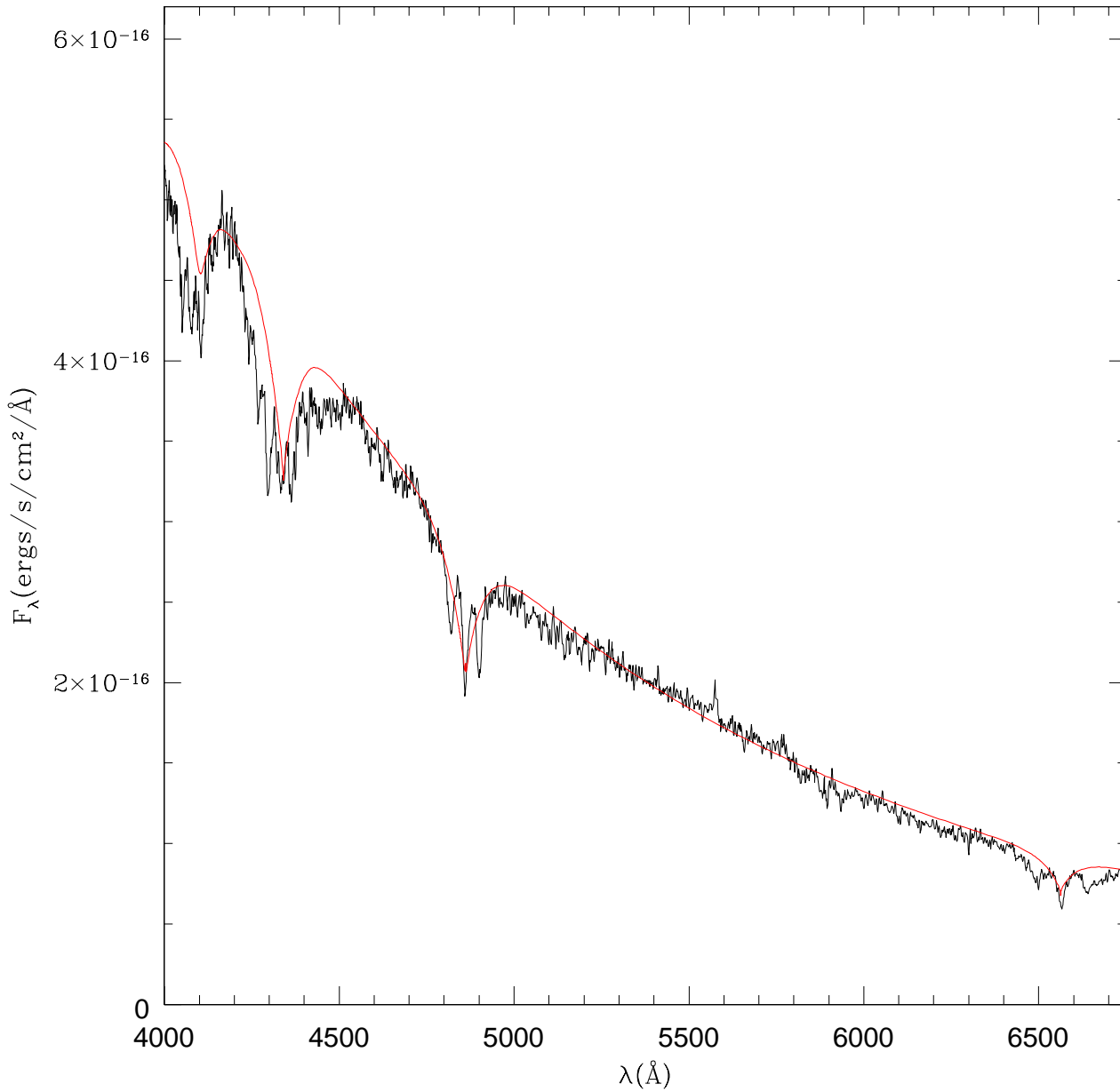


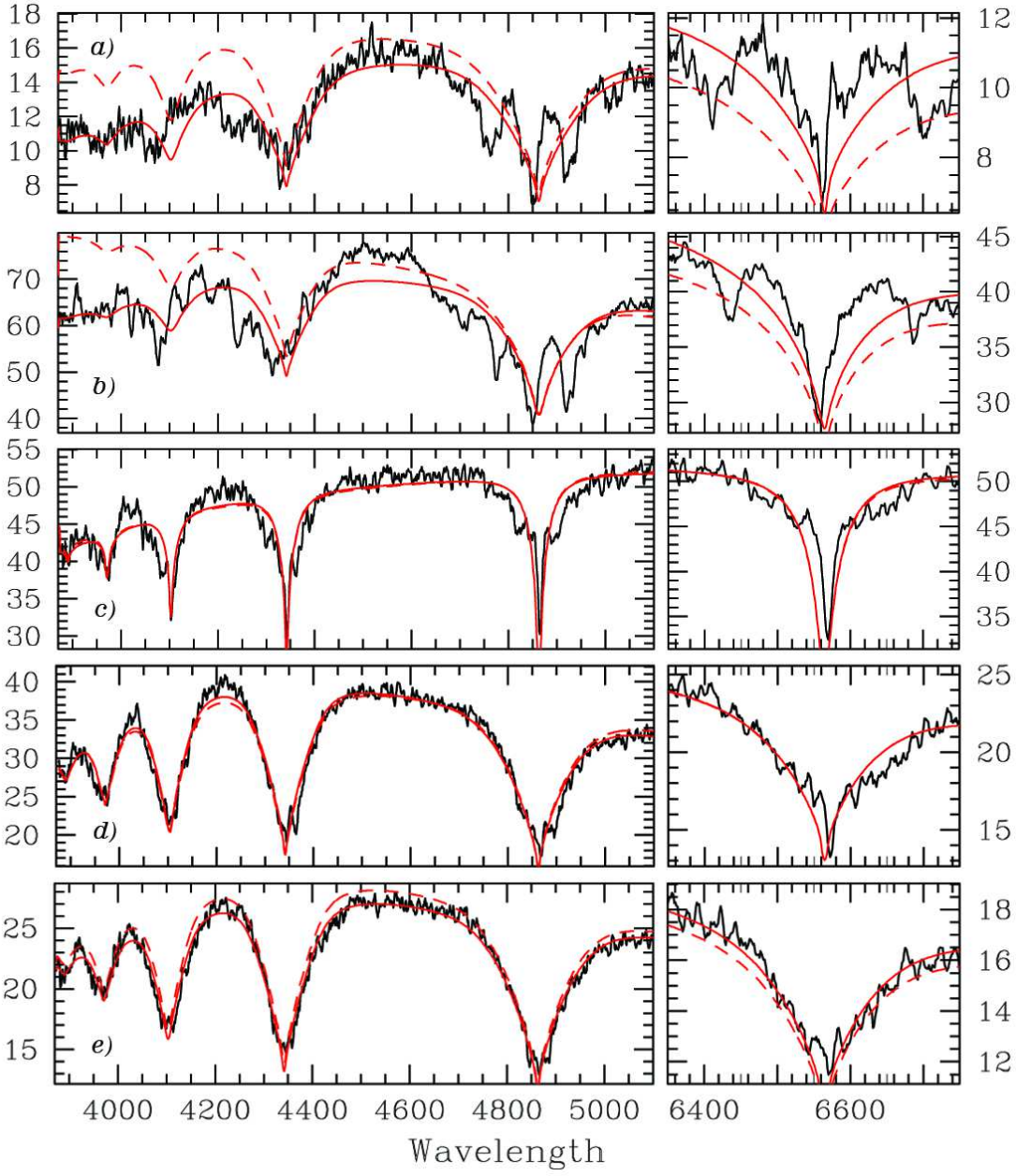
**Figure 1.** SDSS spectrum of one of the stars we identified Zeeman splittings, SDSS J111010.50+600141.44, indicative of a 6.2 MG magnetic field. A DA model *without magnetic field* of  $T_{\text{eff}} = 36\,000$  K,  $\log g = 9.64$ ,  $M=1.33 M_{\odot}$  results from a least-squares fit to the spectra, plotted in red, obviously inadequate; the lines are wide because of the Zeeman splittings, not due to large pressure (gravity) broadening.

by future observations. Furthermore, any estimate of the overall percentage of magnetic to non-magnetic white dwarf stars needs to take this apparent selection effect into account (Liebert, Bergeron, & Holberg 2003).

### 3.1 Estimation of the Magnetic Field Strength

For fields stronger than 10 kG but weaker than 2 MG, i.e., in the Paschen-Back limit, low level ( $n \leq 4$ ) lines will be split into three components, with the shifted components separated by around

$$\Delta\lambda = \pm 4.67 \times 10^{-7} \lambda^2 B$$



with  $\lambda$  in Ångströms and B in MG (Jenkins & Segrè 1939; Hamada 1971; Garstang 1977). The quadratic splitting is given by

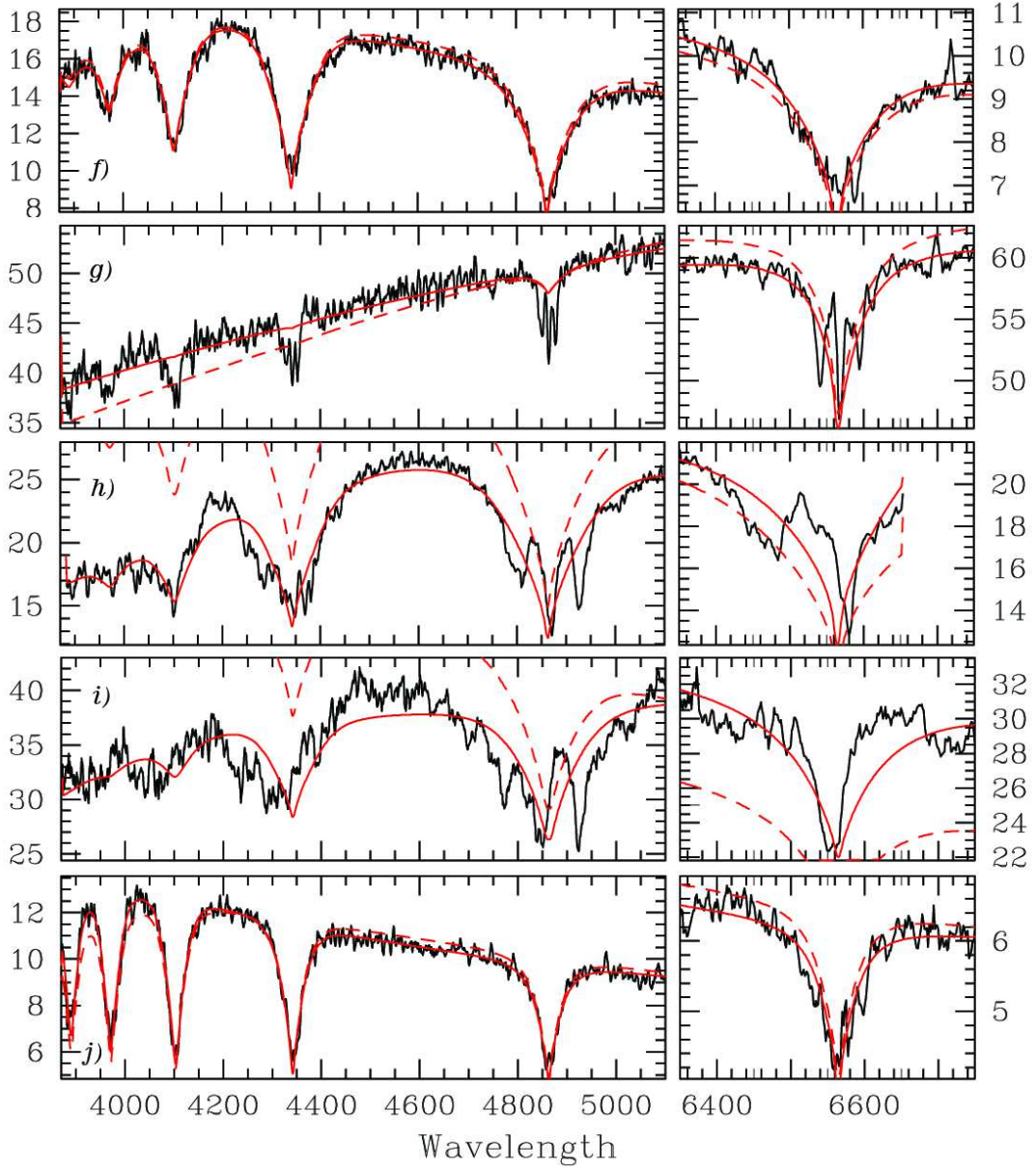
$$\Delta\lambda_q = -\frac{e^2}{a_0^2} 8mc^3 h \lambda^2 n^4 (1 + m_\ell^2) B^2 \simeq -4.97 \times 10^{-23} \lambda^2 n^4 (1 + m_\ell^2) B^2 \text{ Å}$$

where  $a_0$  is the Bohr radius, and  $m_\ell$  the magnetic quantum number. This formula is valid for  $2p$  to  $ns$  and  $2p$  to  $nd$  transitions, where  $n$  is the principal quantum number. For the  $2s$  to  $np$  transitions,

$$\Delta\lambda_q \simeq -4.97 \times 10^{-23} \lambda^2 [n^2(n^2 - 1)(1 + m_\ell^2 - 28) B^2 \text{ Å}$$

Note that because of the  $n^4$  dependency of the quadratic Zeeman splitting, even for fields around 1 MG, the  $n \geq 7$  lines show dominant quadratic splittings (Fig. 5).

For magnetic fields less than  $\simeq 2$  MG, the Zeeman splitting is difficult to observe in low resolution spectra of white dwarfs because the spectral lines are already broadened due to the high density. The linear Zeeman splitting is equivalent to a broadening of unpolarized spectral lines of the order of 10 km/s for fields around 10 kG. For higher fields the magnetic energy cannot be included as a perturbation because the cylindrical symmetry of the magnetic field start to disturb the spherical symmetry of the Coulomb force that keeps the hydrogen atom together. For the  $n = 1$  level, the Lorentz force and



the Coulomb force are of the same order for  $B=4670$  MG. As the energy of the levels is proportional to the inverse of  $n^2$ , the higher levels are disturbed for much smaller fields.

The observed Zeeman splitting represents the mean field across the surface of the star. If the field is assumed as dipole, the mean field is related to the polar field by

$$B = \frac{1}{2} B_p \sqrt{1 + 3 \cos^2 \theta}$$

where  $B_p$  is the polar field and  $\theta$  is the angle between the field and the line of sight. Simple centered dipoles are rarely, if ever, seen in real stars (e.g. Külebi et al. 2009).

To estimate the magnetic fields, we measured the H $\alpha$  and H $\beta$  mean splittings independently and used the mean fields estimated by Külebi et al. (2009) as scale. Our measurements are of the mean line centers, by visual inspection, and therefore do not take into account the shape of the lines, which are different due to the fact the for most stars the magnetic field is not centered at the center of the star (Külebi et al. 2009). Our estimates also ignore any effects due to higher moments than dipoles, or double-degenerate stars. The estimates are therefore very rough, but do indicate the order of magnitude of the magnetic field.

For fields above 30 MG, like for SDSS J085649.68+253441.07 shown in Figure 6, the line identification is difficult, and we adjusted graphically the spectra to the theoretical Zeeman positions only.

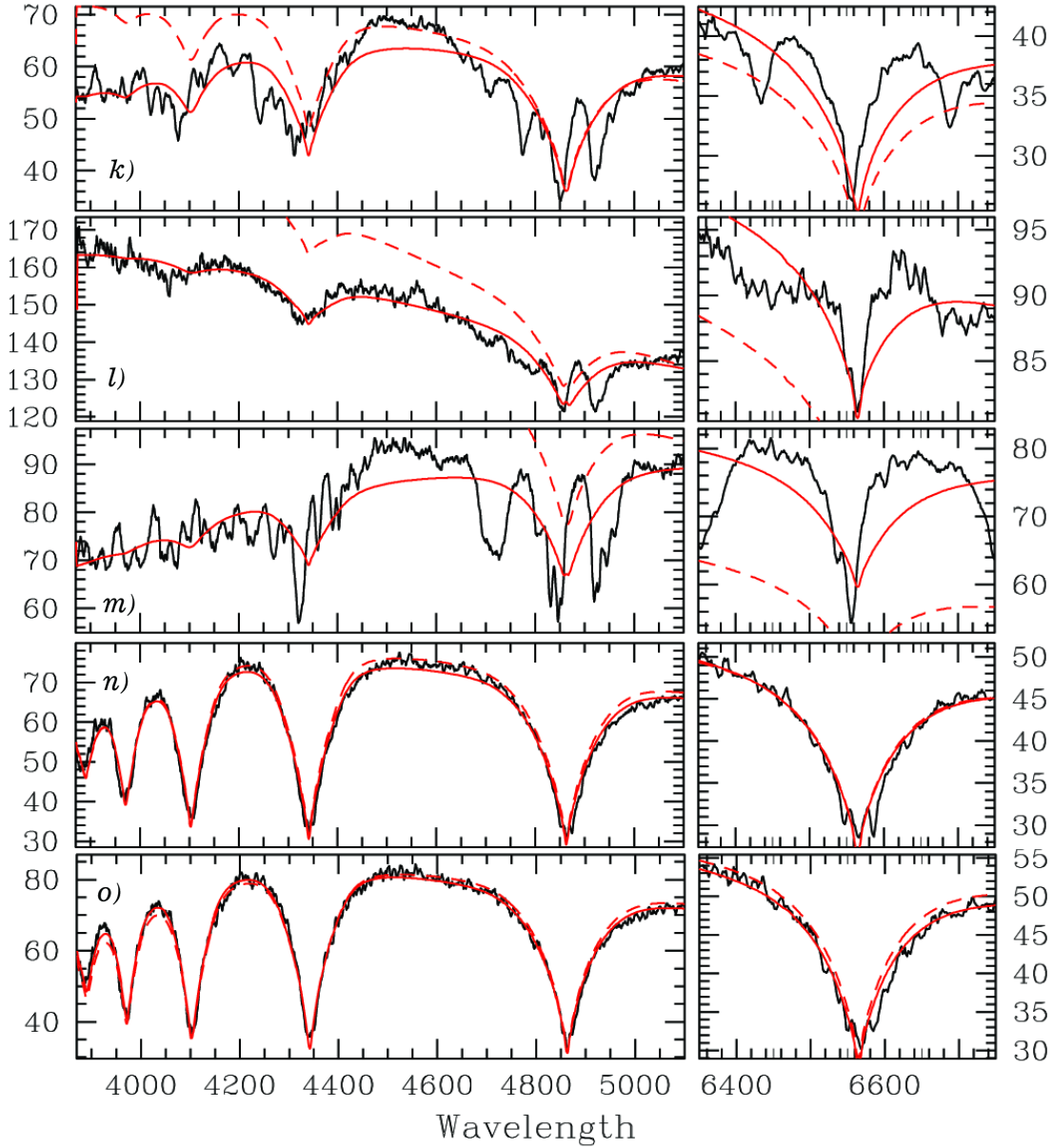


**Figure 2.** Highest S/N SDSS spectra of a sample of stars for which we identified Zeeman splittings indicative of fields from 14 MG to 1.3 MG magnetic fields. a) Plate-MJD-Fiber=1954-53357-393, 13 MG, SDSS J101428.10+365724.40, b) 0415-51879-378, 11 MG, J033145.69+004517.04, c) 1616-53169-423, 2.4 MG, 123414.11+124829.58, d) 2277-53705-484, 2.2 MG, 083945.56+200015.76, e) 2772-54529-217, 2.2 MG, 141309.30+191832.01, f) 2694-54199-175, 1.7 MG, 064607.86+280510.14, g) 2376-53770-534, 2.6 MG, 103532.53+212603.56, h) 2417-53766-568, 9.9 MG, 031824.20+422651.00, i) 2585-54097-030, 14 MG, 100759.81+162349.64, j) 2694-54199-528, 1.3 MG, 065133.34+284423.44, k) 0810-52672-391, 11 MG, 033145.69+004517.04, l) 1798-53851-233, 14 MG, 131508.97+093713.87, m) 2006-53476-332, 19 MG, 125715.54+341439.38, n) 2644-54210-167, 1.9 MG, 121033.24+221402.64, o) 2430-53815-229, 2.5 MG, 085106.13+120157.84. DA models without magnetic field results from least-squares fits to the spectra are plotted in red, obviously inadequate.

Fig. 7 shows fits of centered dipole magnetic models with  $\log g = 8.0$  as those by Külebi et al. (2009) for 5 stars, to illustrate the discrepancies of assuming centered fields. Table 1 shows the estimated values for the magnetic fields for the 521 spectra we measured. The 5th column of the table shows the signal-to-noise ratio in the region of the  $g$  filter of the spectra,  $S/N(g)$ .

Fig. 8 shows the distribution of fields for our sample, showing an increase in the number of stars for lower fields, except for the lowest bin, where selection effects are important, as our  $R \simeq 2000$  resolution implies we cannot detect  $B \leq 2$  except at the highest S/N.

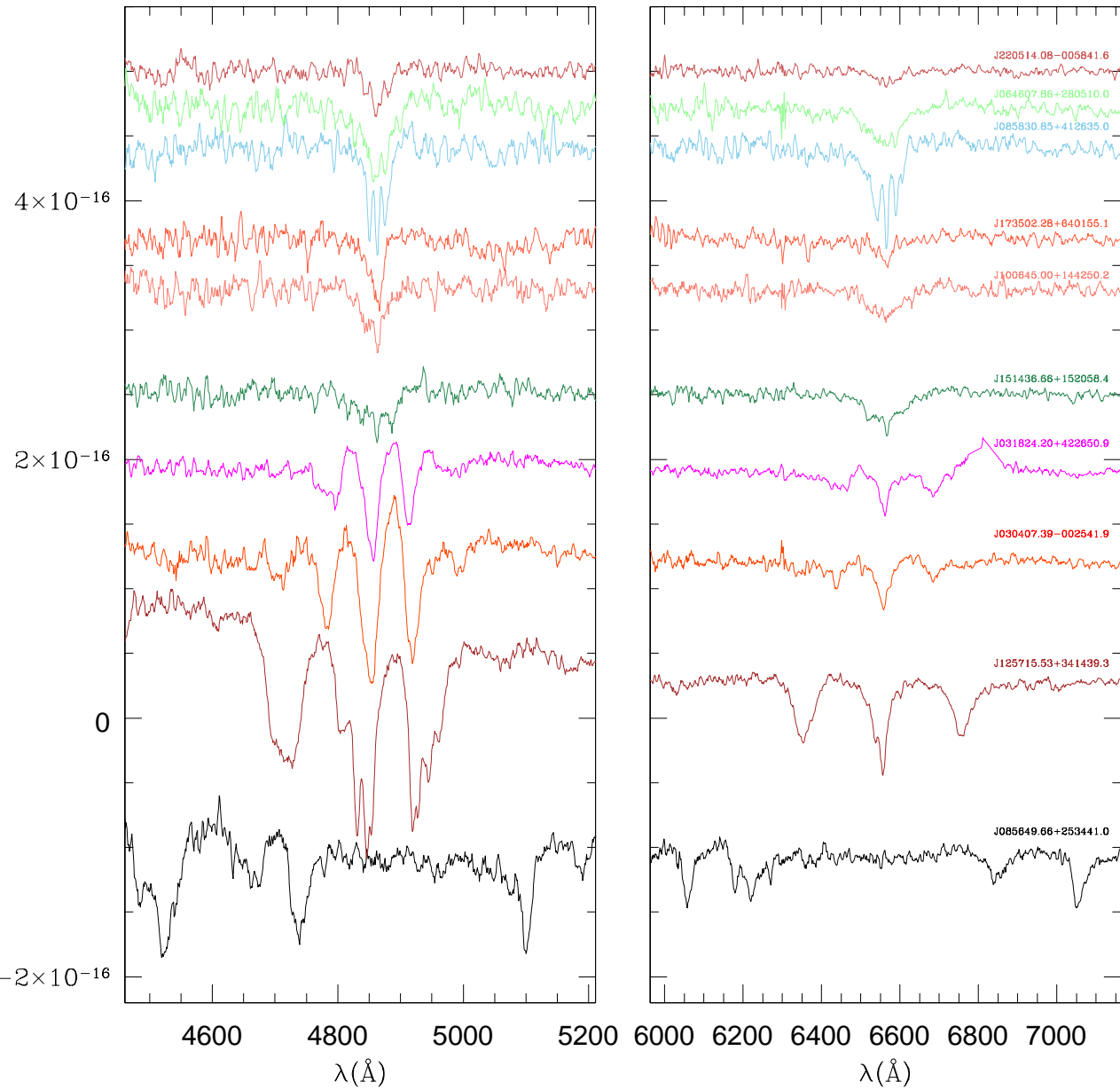


**Figure 3.** H $\beta$  (left-hand panel) and H $\alpha$  (right-hand panel) line profiles for a sample of new magnetic white dwarf stars, with fields of  $\simeq 3$  MG at the top, and 90 MG at the bottom. The y-column shows flux in arbitrary units.

#### 4 BLIND TEST

In order to check whether magnetic white dwarfs can be identified and analyzed with sufficient confidence using noisy spectra, we have performed a blind test. One group has calculated model spectra for white dwarfs with and without magnetic fields for effective temperatures between 8000 and 40000 K and  $\log g = 8.0$ . For the models with magnetic fields we assumed centered magnetic dipoles with a polar field strength between 1 and 550 MG and viewing angles between the observer and the magnetic fields between 0 and 90°. Subsequently, we added Gaussian noise with signal-to-noise ratios between 4 and 35.

In total 346 such spectra were given to the second group whose task it was to identify which of the objects were magnetic and what the mean magnetic field strength was. This group did not know how many of the spectra were calculated assuming no magnetic fields and what the assumed field strength for the magnetic objects were.

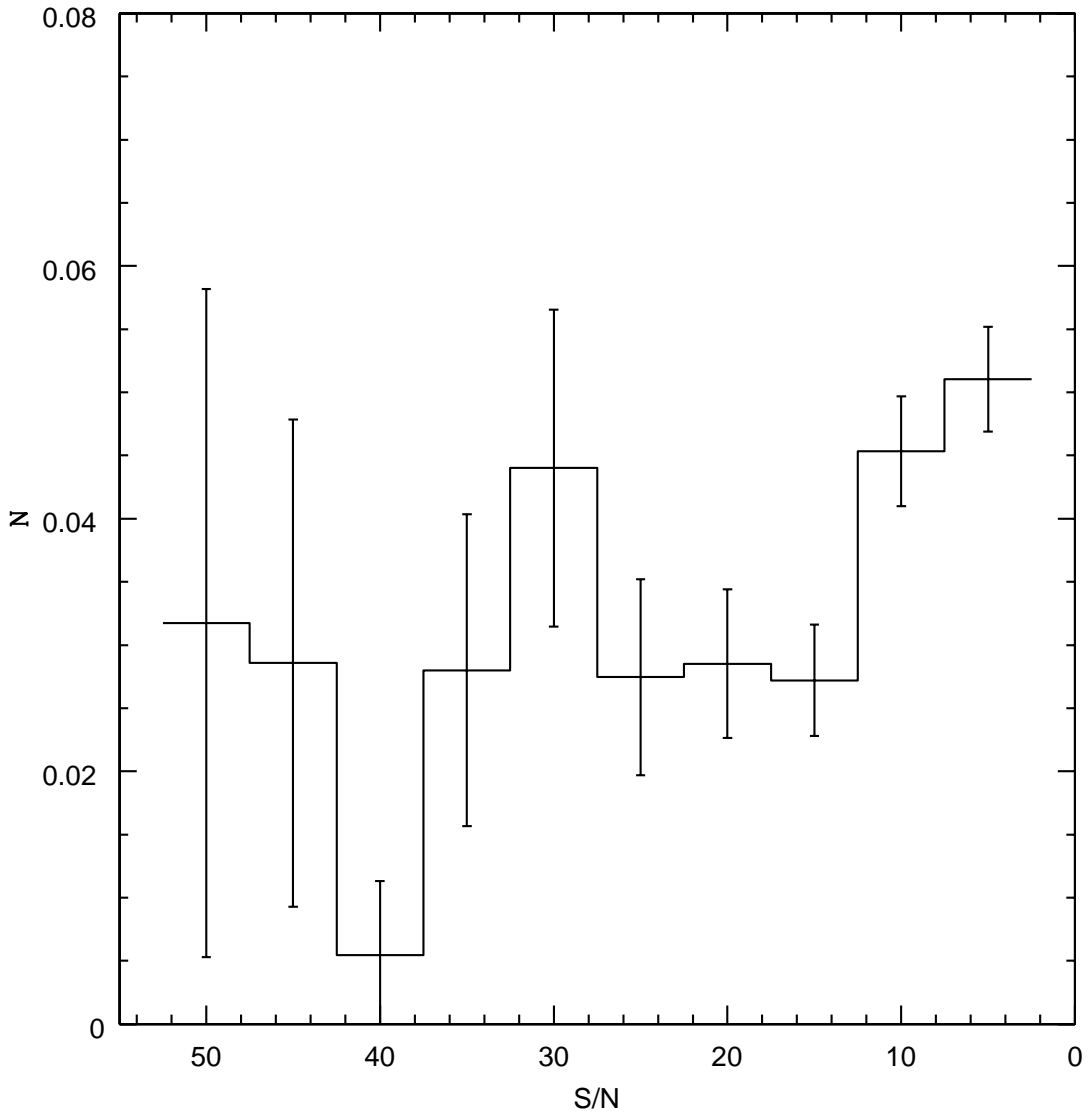


**Figure 4.** Fraction of detected magnetic DA white dwarfs versus S/N of the spectra.

To be on the secure side, we assumed that all objects with a magnetic field lower than 2 MG were regarded as non magnetic.

79 of the 346 noisy spectra were based on zero-field models ( $< 2 \text{ MG}$ ). Only seven of them were wrongly classified as being magnetic and all of them had signal-to-noise ratios below eight; in total we have simulated 43 objects with  $\text{S/N} < 8$ . None of the false detections had a determined field strength above 3 MG so that no non-magnetic white dwarf was regarded as having a strong magnetic field. If we disregard detections below 2 MG and signal-to-noise ratios below 10 we do not detect any false-magnetics.

41 of the noisy theoretical spectra were assigned to be non-magnetic by the second group but in fact had assumed magnetic fields larger than 2 MG. This number is indeed significantly large because we had in total 130 objects with simulated zero fields. At  $B < 50 \text{ MG}$  13 out of 265 objects (5%) were false-negatives. At  $B > 50 \text{ MG}$  we have 28 out of 81 objects (34% false) false negatives. The distribution between 50 and 400 MG is quite flat. If we limit ourselves to signal-to-noise ratios above ten the number of false-negatives is reduced to seven objects (out of 84) which all had relatively weak features (magnetic fields above 100 MG and effective temperature above 35000 K). At  $\text{S/N} > 15$  this number is further reduced to two (out of 52) objects; at  $\text{S/N} > 20$  (34 simulated objects) all simulated magnetic objects were determined as such.

The determined mean field strengths were compared to the mean magnetic fields of the dipole models. 214 of the theoretical spectra were calculated for field strength between 1 and 100 MG. If we again limit ourself to the ones with signal-to-noise

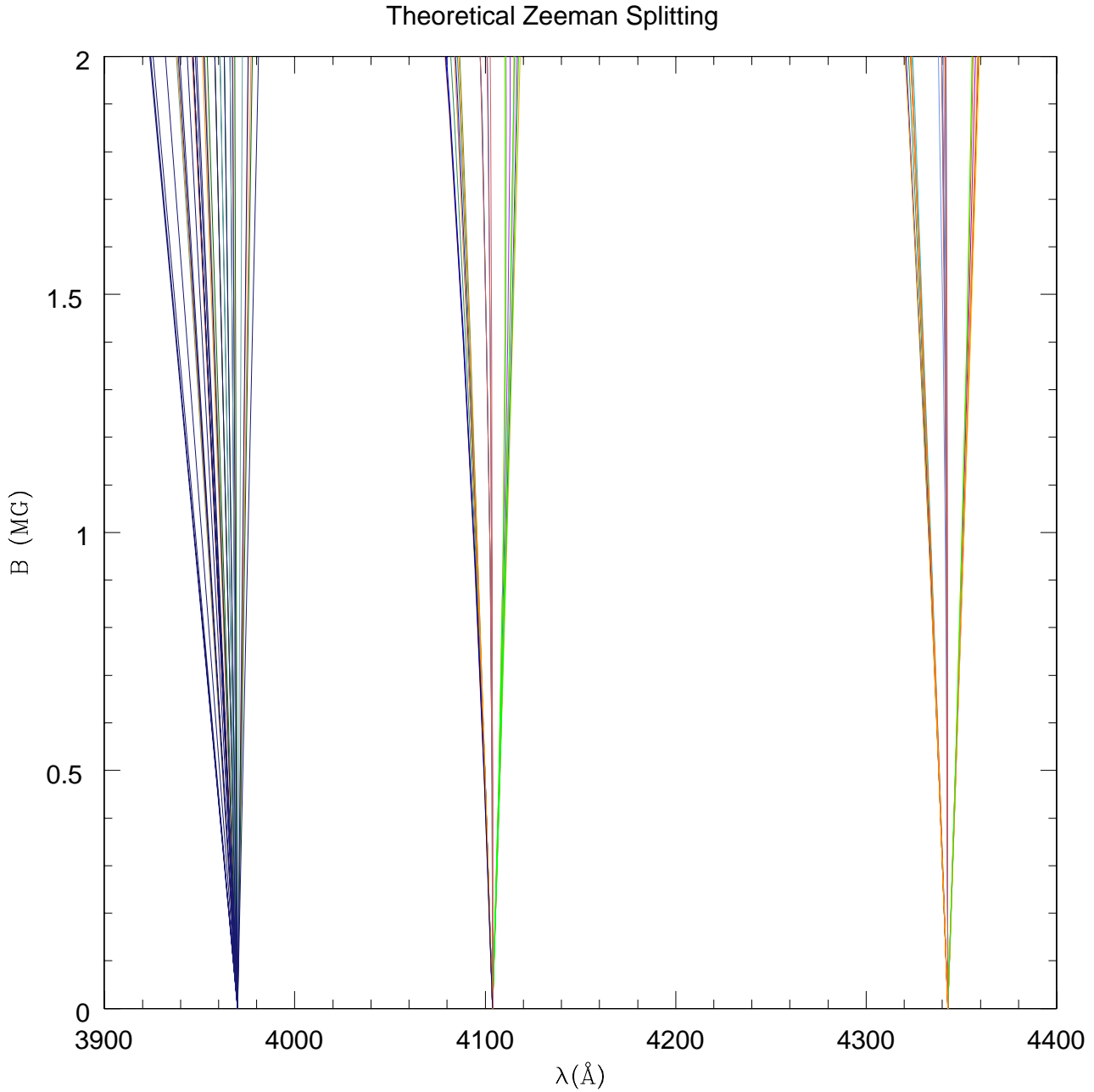


**Figure 5.**  $\text{He}, n=7 \rightarrow 2, \lambda_0 = 3971 \text{ \AA}$  (left) to  $\text{H}\gamma, n=5 \rightarrow 2, \lambda_0 = 4342 \text{ \AA}$  (right) theoretical Zeeman splittings for  $B=0 \rightarrow 2 \text{ MG}$ , showing the higher lines split into multiplets even for these low fields, because the quadratic Zeeman splitting is proportional to  $n^4$ .

ratios above ten, the magnetic field determination “by eye” was rather accurate. In only six cases the determined magnetic field strength differed from the simulated one by more than a factor of two.

At field above 100 MG (53 simulated spectra) the magnetic-field determination was less satisfactory even at signal-to-noise ratios above 15. The magnetic fields were often wrong (mostly underestimated) by more than a factor of two.

Without detailed modeling, the magnetic field determination at very high magnetic fields ( $> 100 \text{ MG}$ ) is much more difficult than at lower fields. This is because most of the spectral lines are completely washed out by the quadratic Zeeman effect if the magnetic field varies over the stellar surface (this variation amounts to a factor of two in the case of dipole models). Only the so-called stationary line components for which the wavelengths go through maxima or minima as functions of the magnetic field strength remain visible. The corresponding field strength is not necessarily close to the mean field strength. This could partially explain the difference between the field determinations “by eye” and the simulated values.

We conclude that we can distinguish between spectra from magnetic ( $> 2 \text{ MG}$ ) and non-magnetic white dwarfs ( $\leq 2 \text{ MG}$ )

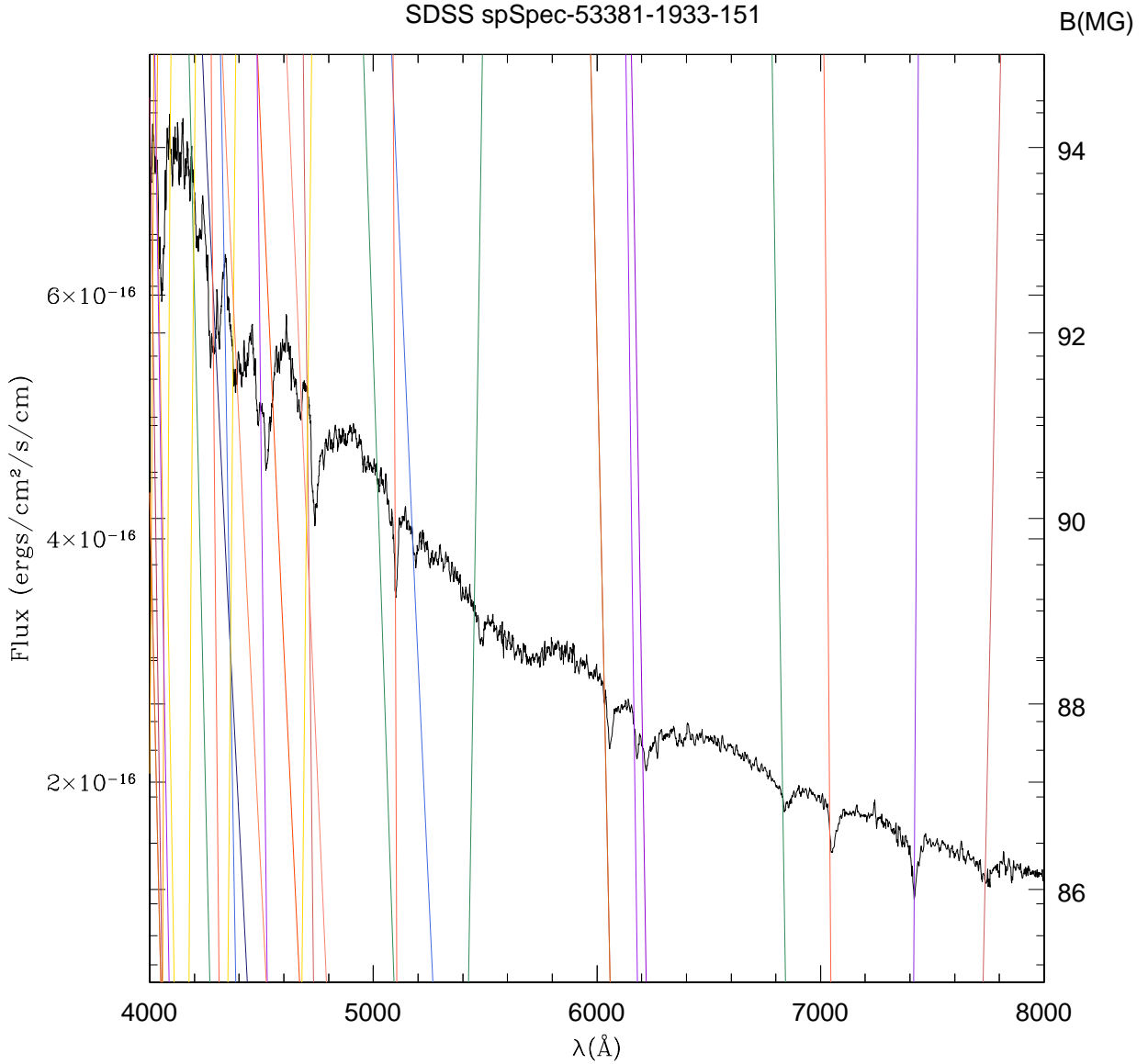


**Figure 6.** Spectrum for SDSS J085649.68+253441.07 DA with a magnetic field around 90 MG, and the position of the theoretical Zeeman splittings (continuous colored lines) for a dipole magnetic field B indicated on the right of the plot.

with very high confidence if we limit ourselves to spectra with signal-to-noise ratios above 10. Hot magnetic white dwarfs with effective temperatures above 35000 K and fields above 100 MG can be missed due to their shallow features. For field strength above 100 MG we generally have to assume large uncertainties in the “by eye” field determination.

## 5 VARIABLE FIELDS

For eleven stars we have from two to six independent co-added spectra, obtained at different epochs, and for a few of them we could see significant changes in the Zeeman splittings, probably due to an inclined magnetic field axis with respect to the rotational axis of the star. For SDSS 030407-002541.74, for example, shown in Fig. 9, the structure of the Zeeman splitting changes substantially, indicating either a very complex magnetic structure, or possibly a double degenerate magnetic system. We do not have time series spectra to study their variability timescale, but such changes in the line profiles have been detected for other magnetic white dwarfs, due to rotation (e.g. Burleigh, Jordan, & Schweizer 1999; Euchner et al. 2002, 2005, 2006). Breedt et al. (e.g. 2012) shows some of the magnetic white dwarfs are in fact white dwarf binaries, when phase resolved spectra are obtained.

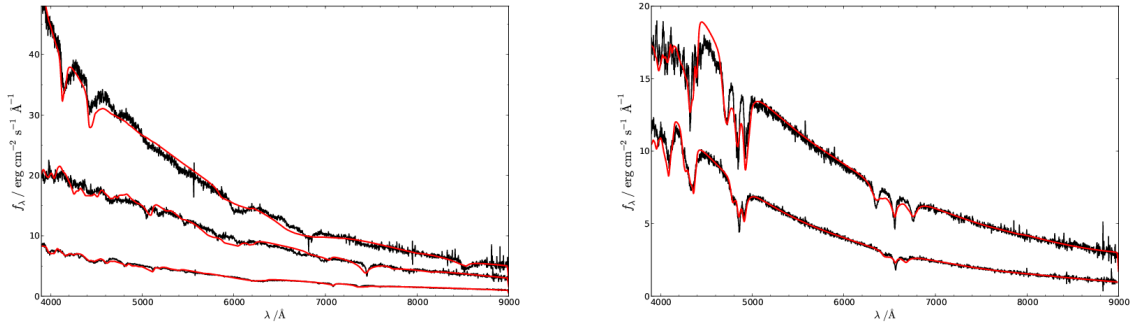


**Figure 7.** Sample fits done to 5 different objects using the method from Külebi et al. (2009), with the database of centered dipolar models. The plots include the following observed spectra (black lines) with the best fit dipole models (in red lines): (first part) SDSS J135141.13+541947.35 with ( $B_p = 500$  MG), SDSS J021148.22+211548.19 ( $B_p = 168$  MG), SDSS J101805.04+011123.52 ( $B_p = 127$  MG); (second part) SDSS J125715.54+341439.38 ( $B_p = 12$  MG), SDSS J074853.08+302543.56 ( $B_p = 6.8$  MG). The fits are intended to be representative and the disagreements between model and fits are due to a lack of detailed modeling in which effective temperature and the sophisticated magnetic models has not been accounted for. In the plots, arbitrary factors of normalization have been used for display.

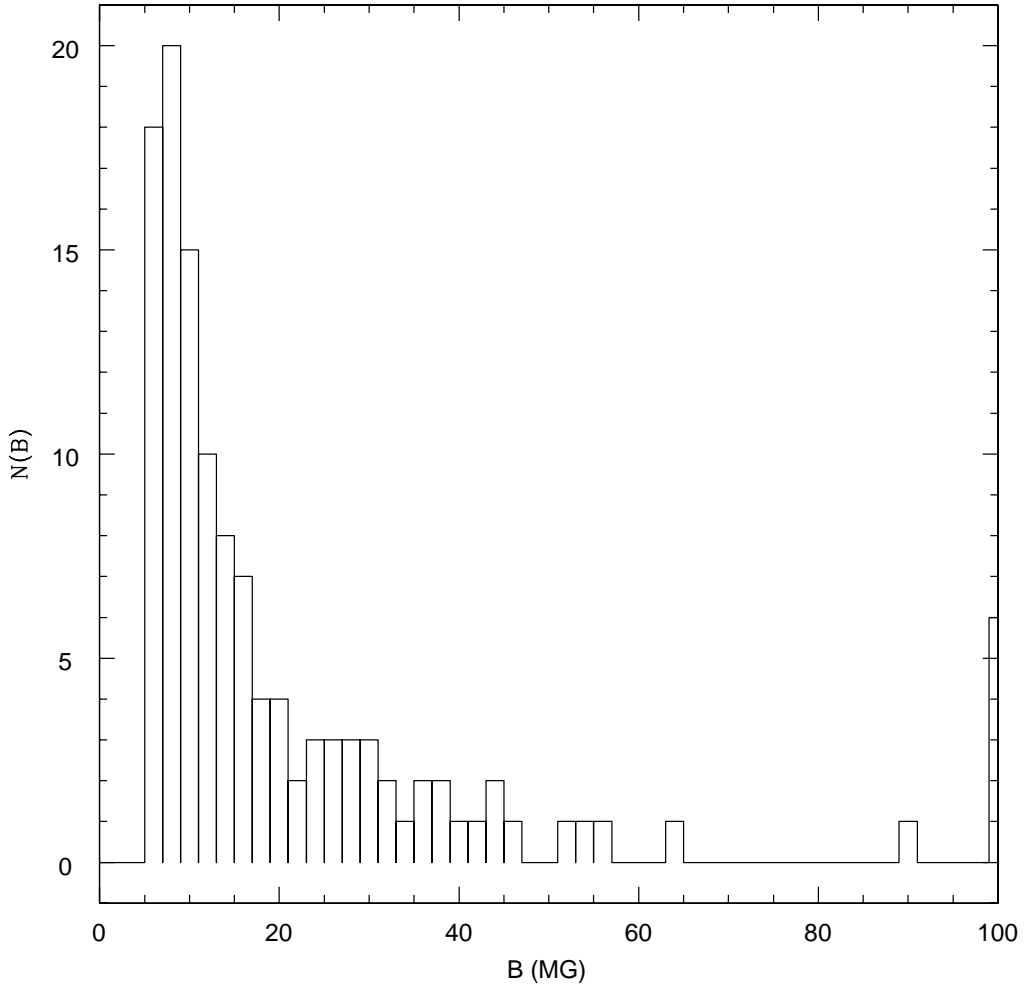


**Figure 8.** Number of white dwarfs versus magnetic field for the SDSS sample. As our detection limit is around 1–2 MG, selection effects in the lowest bin are important.

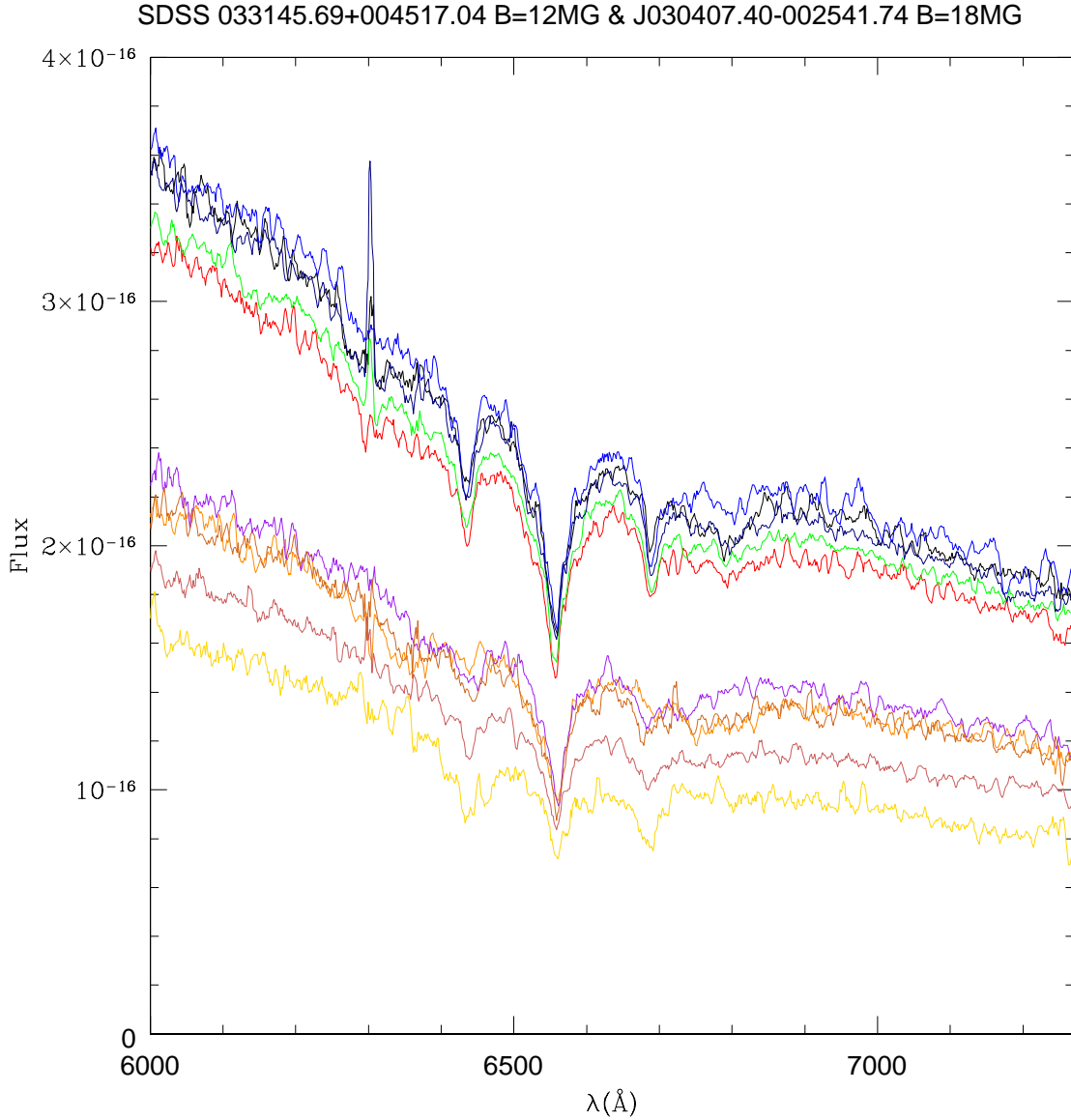


**Figure 9.** Spectra for different epochs for SDSS J033145.69+004517, with B=12 MG (top), and SDSS J030407.40-002541.74, with B=18 MG. The last star set of spectra shows significant changes in the Zeeman splittings with time. The spectra are not purposefully offset from each other.

## 6 THE EFFECT OF MAGNETIC FIELD ON MASS ESTIMATES

The mass distribution of the hydrogen-rich DAs shows an effect, which is well-documented since many years, but still not fully understood: the average mass, as estimated by the surface gravity, increases apparently below 13 000K for DAs (Bergeron, Saffer, & Liebert 1991; Koester 1991; Kleinman et al. 2004; Liebert, Bergeron, & Holberg 2005; Kepler et al. 2007; Limoges & Bergeron 2010; Gianninas et al. 2010; Tremblay, Bergeron, & Gianninas 2011; Gianninas, Bergeron, & Ruiz 2011). Single white dwarf masses in these studies are typically determined through spectroscopy - measuring line widths due to Stark and neutral pressure broadening. Mass determinations from photometry, and gravitational redshift (Engelbrecht & Koester 2007; Falcon et al. 2010) do not show this mass increase, so the increase is probably not real, and merely reflects some failure of the input physics in our spectroscopic models. Efforts have been made to improve the treatment of the line broadening (Koester et al. 2009; Tremblay et al. 2010), but the apparent mass increase remains (Gianninas et al. 2010; Tremblay, Bergeron, & Gianninas 2011; Gianninas, Bergeron, & Ruiz 2011). In Fig. 10 we show the masses for DAs with  $S/N \geq 15$  spectra in Kleinman et al. (2013).

Other proposed explanations for the broadening were the treatment of the hydrogen level occupation probability, or convection bringing up subsurface He to the atmosphere, increasing the local pressure. However, no evidence for the He could

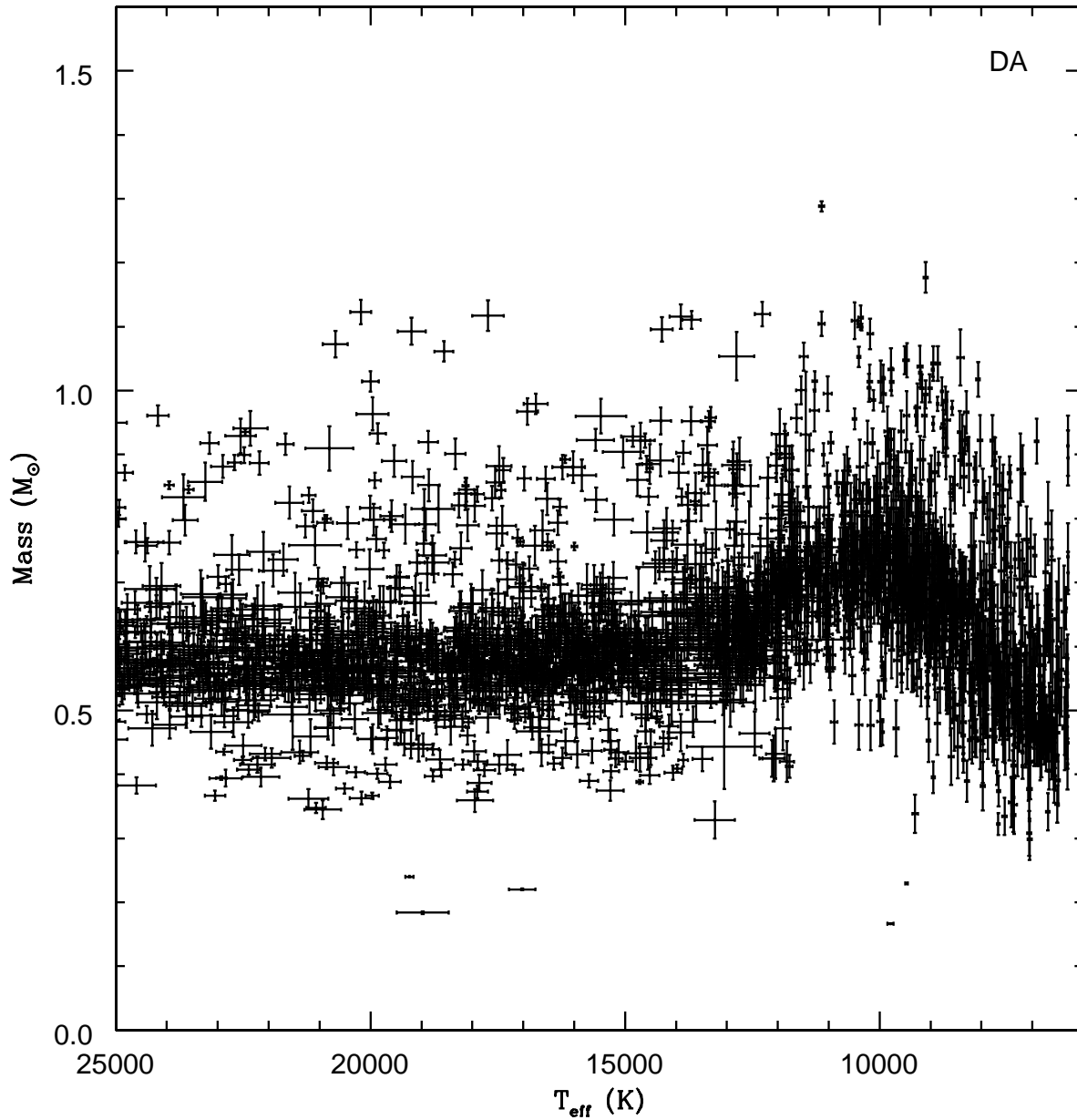


**Figure 10.** Masses for DA stars measured from the  $S/N \geq 15$  SDSS optical spectra by Kleinman et al. (2013), showing the apparent increase in the derived masses around  $T_{\text{eff}} \leq 13000$  K, which are not seen in the masses derived by colors or gravitational redshift.

be found, leaving the very description of convection with the usual mixing length approximation as the most likely culprit (Koester et al. 2009; Tremblay et al. 2010). Calculations using realistic 3D simulation of convection seem to confirm this assumption (Tremblay et al. 2011a).

In this study we explore a complementary possibility for the broadening of the spectral lines below  $T_{\text{eff}} \simeq 13000$  K, the presence of weak magnetic fields in the cooler white dwarfs. Unresolved Zeeman splitting can increase the apparent line widths and mimic a stronger Stark broadening, specially for the higher lines. Since the spectroscopic gravity determination is based on the line widths, an average mass white dwarf star with a weak magnetic field can appear spectroscopically indistinguishable from a non-magnetic, massive star. The combined effect of electric and magnetic fields on the spectral lines is very complicated and has been studied only for special cases of the geometry (e.g. Friedrich et al. 1994; Külebi et al. 2009). Detailed model grids, which include also the effect of the magnetic field on the radiative transfer are therefore not yet available. We find

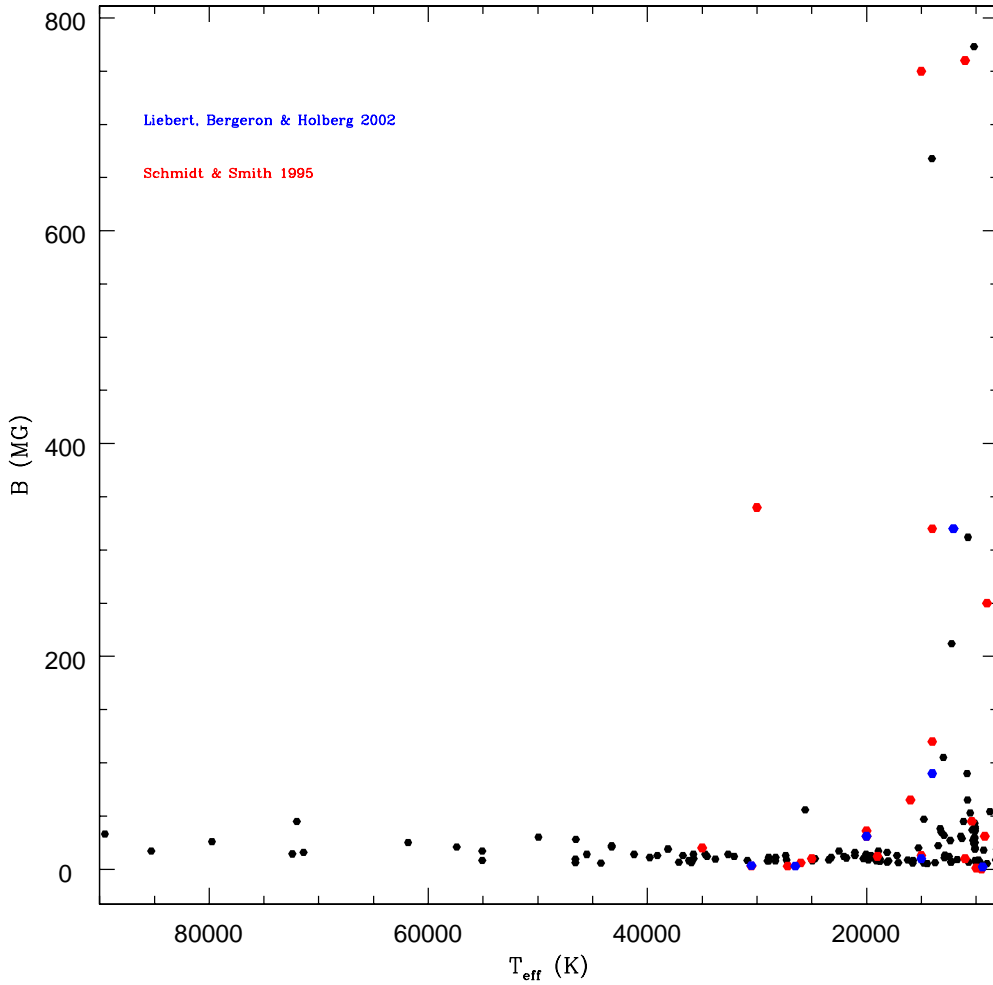


**Figure 11.** Magnetic field versus effective temperature for the SDSS sample, Liebert, Bergeron, & Holberg (2003), and Schmidt & Smith (1995), showing an increase in field for  $T_{\text{eff}} \leq 13\,000$  K, where a surface convection zone develops. As the number of stars is larger at lower temperatures just because they cool on a longer timescale, the fraction of higher field stars is the important parameter.

an increase in the mean field around the same temperature when these stars develop a surface convection zone, raising the possibility that the surface convection zone is amplifying an underlying magnetic field (Figures 11 and 12).

As the Zeeman splitting broadens the lines, we cannot use the line profiles to estimate their surface gravity directly. For fields stronger than  $B \simeq 1$  MG, the magnetic splittings for the  $n=7-10$  energy levels of hydrogen washes out the lines, just like high gravity does. As shown in Fig. 5 the theoretical Zeeman splittings for the Balmer lines initiating at  $n=7$  ( $\text{He}$ ,  $\lambda_0 = 3971$  Å) to  $n=5$  ( $\text{H}\gamma$ ), showing the higher lines split into multiplets even for fields below  $B = 1$  MG. Unfortunately there are no published calculations of the splittings for hydrogen levels higher than  $n=7$  for these fields, where perturbation theory is no longer applicable (Jordan 1992; Ruder et al. 1994). For these higher levels, the Zeeman splittings calculations need higher order terms even for fields of the order of 1 MG.

As we detected Zeeman splitting in the disk integrated spectra for 4% or more of white dwarfs, which comes from global organized fields, perhaps even smaller or unorganized fields are the cause for the line broadening on these cooler stars.

It will be necessary to investigate if surface convection amplification of an underlying weak magnetic field is causing broadening of the spectral lines of white dwarf stars cooler than 13 000 K, leading to misinterpretation of these stars as more massive stars.

Even weaker magnetic fields in white dwarfs have been studied by Koester et al. (1998), who obtained high resolution spectra measurements of the NLTE core of  $\text{H}\alpha$  for 28 white dwarf stars to measure their projected rotational velocities, finding 3 magnetic white dwarfs, and no fields above 10-20 kG for the other stars, all hotter than 14 000 K. Koester et al. (2009a) observed about 800 white dwarfs in the SPY survey, finding 10 magnetic, with fields from 3 to 700 kG. Kawka & Vennes (2012)

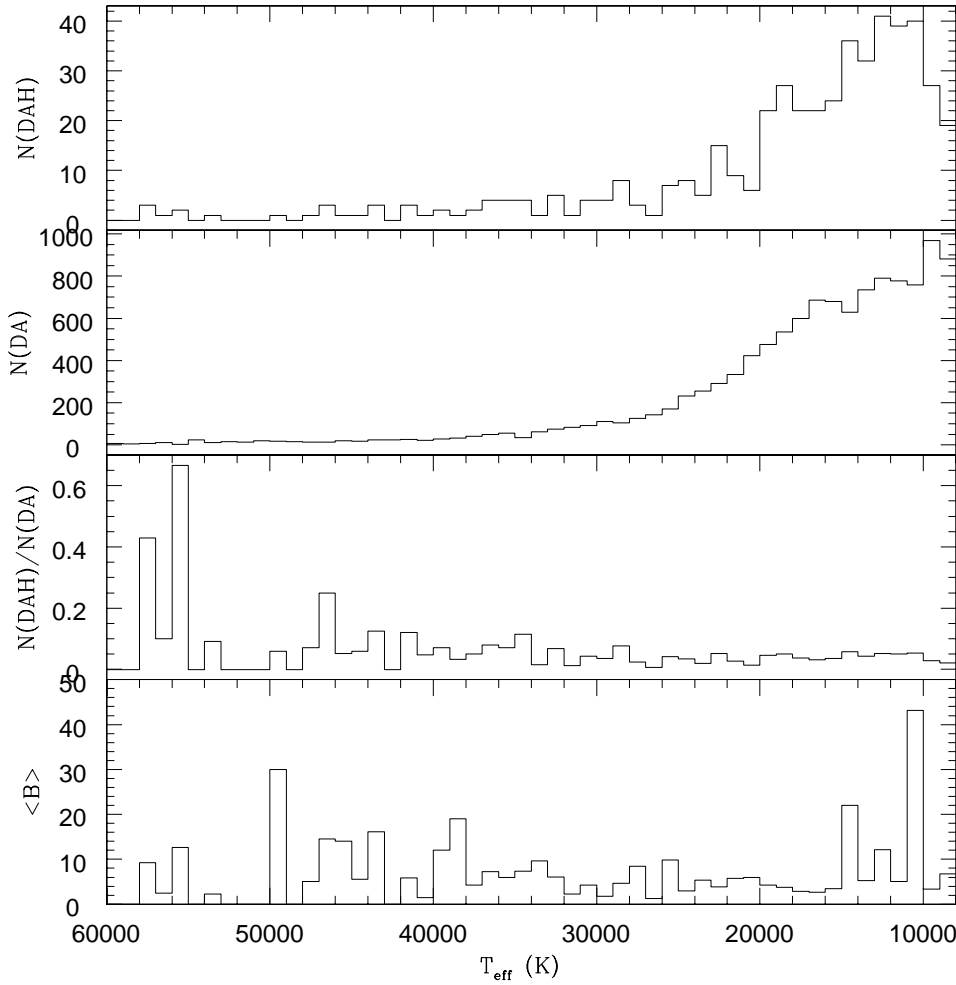


**Figure 12.** The two top panels show the number of DAHs and DAs versus  $T_{\text{eff}}$ . The third panel from the top shows the ratio of the number of DAHs to DAs. On the lowest panel, we see the mean field for DAHs of that  $T_{\text{eff}}$ , showing that even though the fraction of magnetic to non-magnetic measured with  $B > 2$  MG did not increase at lower  $T_{\text{eff}}$ , the mean field does increase.

studied 58 white dwarfs with ESO/VLT/FORS1 spectropolarimetry and estimate 5% of white dwarfs with fields 10 to 100 kG. Landstreet et al. (2012) estimate that 10% of all white dwarf stars have kG fields from ESO/VLT/FORS spectropolarimetry.

## 7 MEAN MASSES

Wickramasinghe & Ferrario (2005) quote a mean mass of  $0.93 M_{\odot}$  for magnetic white dwarfs, based on Liebert, Bergeron, & Holberg (2003) determinations, but the sample includes only a handful of stars with astrometric measured masses, so the evidence that the magnetic white dwarfs are more massive than the average were scarce. Kawka et al. (2007) obtained a mean mass of  $0.78 M_{\odot}$  for the 28 magnetic DA white dwarfs with mass estimates, mainly from fitting the line wings of the spectra.

We estimated the masses for every star with  $S/N_g \geq 10$  spectra, from their  $u, g, r, i, z$  colors, shown in Figure 13, obtaining for the 84 hydrogen-rich magnetic white dwarfs (DAHs) with  $B \leq 3$  MG,  $\langle M \rangle = (0.68 \pm 0.04) M_{\odot}$ . For the 71 DAHs with  $B > 3$  MG,  $\langle M \rangle = (0.83 \pm 0.04) M_{\odot}$ . Figure 14 shows the mass histogram for stars with fields lower and higher than  $B = 3$  MG, compared to nonmagnetic ones, demonstrating there is an increase in the estimated mass for magnetic stars, but the estimated mass values are uncertain because the  $u$  color is severely affected by magnetic fields, caused by the  $n^4$  dependency of the splittings (e.g. Girven et al. 2010). The estimated masses are much larger than the mean masses for the 1505 bright and hot DA white dwarfs in Kleinman et al. (2013), i.e., those with  $S/N \geq 15$  and  $T_{\text{eff}} \geq 13\,000$  K, for which we did not detect any magnetic field,  $\langle M \rangle_{\text{DA}} = (0.593 \pm 0.002) M_{\odot}$ . Even though we find a higher mass for DAHs, our mean is much smaller than the mean masses quoted for the few previously measured magnetic DAs.

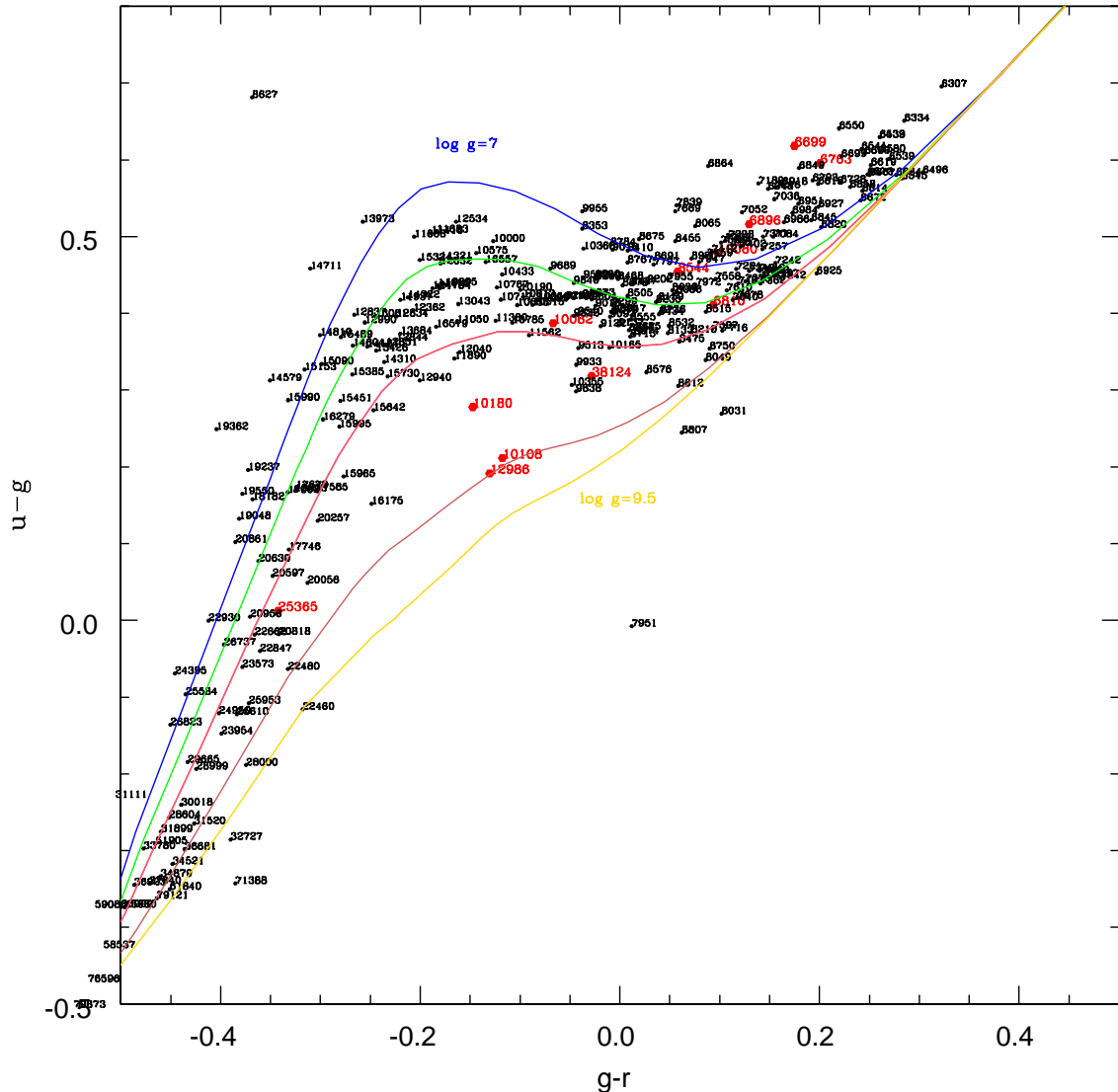


**Figure 13.** Colors for normal DAs (black) and DAHs (red), showing both follow the characteristic curves, but with an excess of DAHs (red) for higher  $\log g$ . We again caution the reader that the  $\log g$  estimates are very uncertain for the magnetic stars because the  $u$  color, where the Balmer jump is located, is heavily affected by the magnetic field.

## 8 DISCUSSION

Considering only spectra with  $S/N \geq 10$ , we increased the number of known magnetic DAs by a factor of 2. We estimated the field strength for 521 stars. Our blind test shows we underestimate the number of magnetics in the simulation and underestimate the field in general. Even for  $S/N \leq 10$ , our candidates have at least a 50% chance of being magnetic, compared to only 4% in field white dwarfs. We showed that the magnetic field changes with time for a few stars we have multiple spectra, pointed that stars with surface temperatures where convection zone develops seems to show stronger magnetic fields than hotter stars, and that the mean mass of magnetic stars seems to be on average larger than the mean mass of non-magnetic stars.

If the apparent increase in masses shown in Fig. 10 were only caused by magnetic field amplification when the surface convection zone appears around  $T_{\text{eff}} \lesssim 13\,000$  K, it should, perhaps, continue to rise at lower temperatures. But if the mass of the convection zone becomes high enough that its kinetic energy is of the same order as the magnetic energy, amplification will not be effective.

Zorotovic, Schreiber, & Gänsicke (2011) estimate the mean WD mass among CVs is  $\langle M_{\text{CV}} \rangle = (0.83 \pm 0.23) M_{\odot}$ , much larger than that found for pre-CVs,  $\langle M_{\text{PCV}} \rangle = (0.67 \pm 0.21) M_{\odot}$ , and single white dwarfs. Are all the magnetic white dwarfs descendant of binaries?

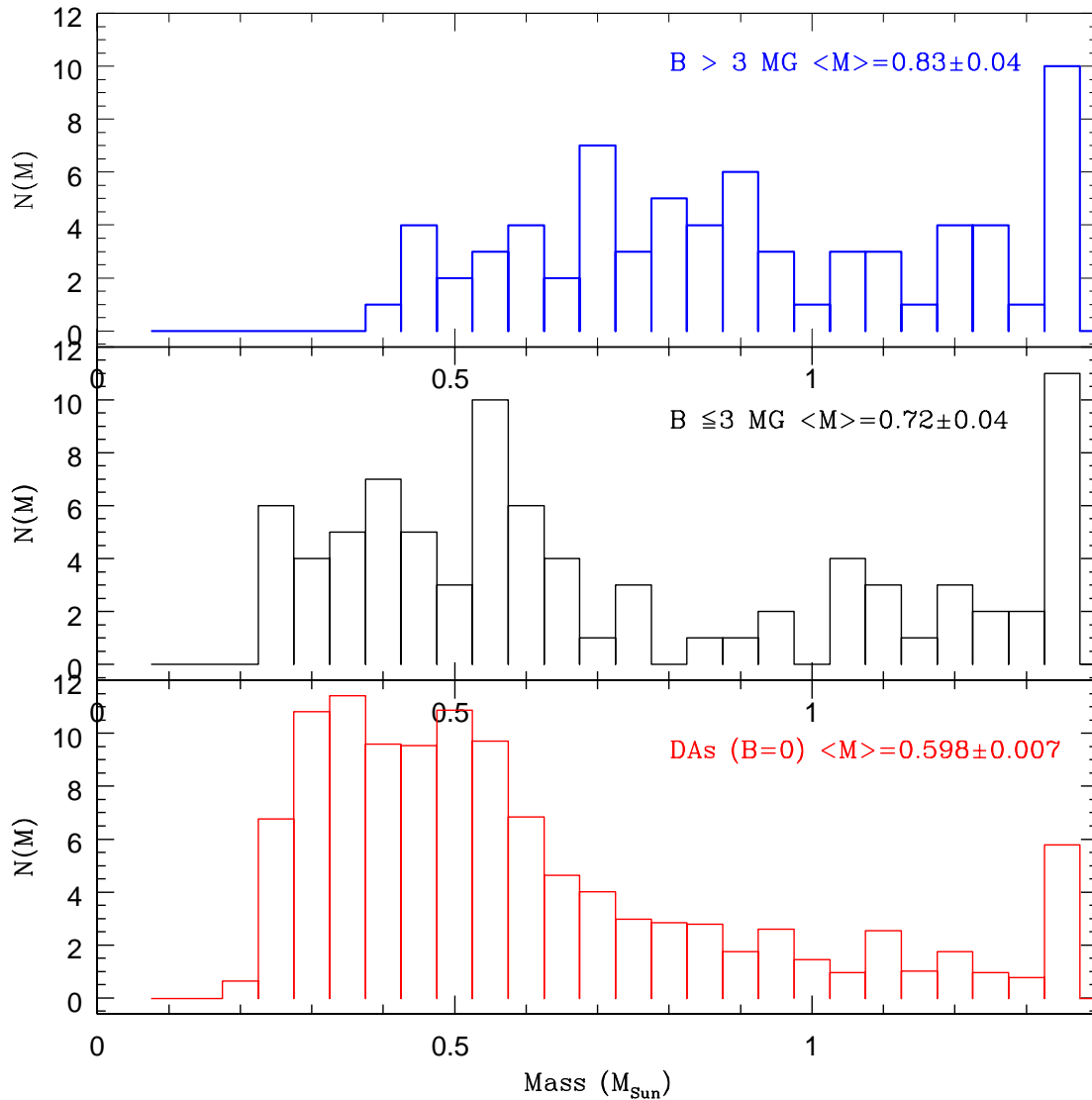


**Figure 14.** Mass histogram from colors for low field (black) and higher field (blue) DAHs and DAs, showing the apparent masses increase with increasing magnetic field.

The Gaia mission will provide parallaxes for all these objects and thereby obtain strong constraints on magnetic and convection models and get an independent check of the surface gravity ( $\log g$ ) determinations, if we assume a mass-radius relation.

## ACKNOWLEDGMENTS

S.O. Kepler, J.E.S. Costa, I. Pelisoli, and V. Peçanha are supported by CNPq and FAPERGS-Pronex-Brazil. BGC is supported by the Austrian Fonds zur Förderung der wissenschaftlichen Forschung through project P 21830-N16. BK is supported by the MICINN grant AYA08-1839/ESP, by the ESF EUROCORES Program EuroGENESIS (MICINN grant EUI2009-04170), by the 2009SGR315 of the Generalitat de Catalunya and EU-FEDER funds. D.E. Winget gratefully acknowledge the support of the US National Science Foundation under grant AST-0909107 and the Norman Hackerman Advanced Research Program under grant 003658-0252-2009. A. Kanaan is supported by CNPq. Funding for the SDSS and SDSS-II was provided by the Alfred P. Sloan Foundation, the Participating Institutions, the National Science Foundation, the U.S. Department of Energy, the National Aeronautics and Space Administration, the Japanese Monbukagakusho, the Max Planck Society, and the Higher

Education Funding Council for England. The SDSS Web Site is <http://www.sdss.org/>. The SDSS is managed by the Astrophysical Research Consortium for the Participating Institutions. The Participating Institutions are the American Museum of Natural History, Astrophysical Institute Potsdam, University of Basel, University of Cambridge, Case Western Reserve University, University of Chicago, Drexel University, Fermilab, the Institute for Advanced Study, the Japan Participation Group, Johns Hopkins University, the Joint Institute for Nuclear Astrophysics, the Kavli Institute for Particle Astrophysics and Cosmology, the Korean Scientist Group, the Chinese Academy of Sciences (LAMOST), Los Alamos National Laboratory, the Max-Planck-Institute for Astronomy (MPIA), the Max-Planck-Institute for Astrophysics (MPA), New Mexico State University, Ohio State University, University of Pittsburgh, University of Portsmouth, Princeton University, the United States Naval Observatory, and the University of Washington.

## REFERENCES

- Babcock H. W., 1947a, PASP, 59, 112  
 Babcock H. W., 1947b, ApJ, 105, 105  
 Bergeron P., Saffer R. A., Liebert J., 1991, White Dwarfs, NATO ASI Series 336, eds. G. Vauclair and E. Sion, 75  
 Braithwaite J. & Spruit H. C. 2004, *Nature*, 431, 839  
 Breedt E., Gänsicke B. T., Girven J., Drake A. J., Copperwheat C. M., Parsons S. G., Marsh T. R., 2012, MNRAS, 423, 1437  
 Burleigh M. R., Jordan S., Schweizer W., 1999, ApJ, 510, L37  
 Das U., Mukhopadhyay B., 2012, IJMPD, 21, 11, 1242001  
 Engelbrecht A., Koester D., 2007, ASPC, 372, 289  
 Euchner F., Jordan S., Beuermann K., Gänsicke B. T., Hessman F. V., 2002, A&A, 390, 633  
 Euchner F., Reinsch K., Jordan S., Beuermann K., Gänsicke B. T., 2005, A&A, 442, 651  
 Euchner F., Jordan S., Beuermann K., Reinsch K., Gänsicke B. T., 2006, A&A, 451, 671  
 Falcon R. E., Winget D. E., Montgomery M. H., Williams K. A., 2010, ApJ, 712, 585  
 Friedrich S., Ostreicher R., Ruder H., Zeller G., 1994, A&A, 282, 179  
 García-Berro E., et al., 2012, ApJ, 749, 25  
 Garstang R. H., 1977, RPPh, 40, 105  
 Giannicche N., Bergeron P., Dufour P., 2012, ApJS, 199, 29  
 Gianninas A., Bergeron P., Dupuis J., Ruiz M. T., 2010, ApJ, 720, 581  
 Gianninas A., Bergeron P., Ruiz M. T., 2011, ApJ, 743, 138  
 Girven J., Gänsicke B. T., Külebi B., Steeghs D., Jordan S., Marsh T. R., Koester D., 2010, MNRAS, 404, 159  
 Greenstein J. L., Henry R. J. W., O'Connell R. F., 1985, ApJ, 289, L25  
 Hamada T., 1971, PASJ, 23, 271  
 Holberg J. B., Sion E. M., Oswalt T. D., 2011, AAS, 43, #341.02  
 Jenkins F. A., Segrè E., 1939, PhRv, 55, 52  
 Jordan S., 1992, A&A, 265, 570  
 Jordan S., Aznar Cuadrado R., Napiwotzki R., Schmid H. M., Solanki S. K. 2007, A&A, 462, 1097  
 Kawka, A. et al. 2003, *NATO Science Series II*, 105, 109  
 Kawka A., Vennes S., Schmidt G. D., Wickramasinghe D. T., Koch R., 2007, ApJ, 654, 499  
 Kawka A., Vennes S., 2012, MNRAS, 425, 1394  
 Kepler S. O., Kleinman S. J., Nitta A., Koester D., Castanheira B. G., Giovannini O., Costa A. F. M., Althaus L., 2007, MNRAS, 375, 1315  
 Kemp J. C., 1970, ApJ, 162, L69  
 Kleinman S. J., et al. 2004, ApJ, 607, 426  
 Kleinman S. J., Kepler S.O., Koester D., Pelisoli I., Peçanha V., Nitta A., Costa J.E.S., Krzesiński J., et al. 2013, ApJS, 204, 5.  
 Koester D., 1991, in Proc. 7th European Workshop on White Dwarfs, NATO ASI Ser., ed. G. Vauclair & E. M. Sion (Dordrecht: Kluwer), 343  
 Koester D., 2010, MmSAI, 81, 921  
 Koester D., Dreizler S., Weidemann V., Allard N. F., 1998, A&A, 338, 612  
 Koester D., et al., 2001, A&A, 378, 556  
 Koester D., Kepler S. O., Kleinman S. J., Nitta A., 2009, JPhCS, 172, 012006  
 Koester D., Voss B., Napiwotzki R., Christlieb N., Homeier D., Lisker T., Reimers D., Heber U., 2009, A&A, 505, 441  
 Klebi B., Jordan S., Euchner F., Gänsicke B. T., Hirsch H. 2009, A&A, 506, 1341  
 Kundu A., Mukhopadhyay B., 2012, MPLA, 27, 15, 1250084-1

- Landstreet J. D., Bagnulo S., Valyavin G. G., Fossati L., Jordan S., Monin D., Wade G., 2012, A&A, 545, 30
- Liebert J., Bergeron P., Holberg J. B., 2003, AJ, 125, 348
- Liebert J., Bergeron P., Holberg J. B., 2005, ApJS, 156, 47
- Liebert J., Fleming T. A., Green R. F., Grauer A. D., 1988, PASP, 100, 187
- Limoges M.-M. & Bergeron P. 2010, ApJ, 714, 1037
- Nordhaus J., 2011, PNAS, 108, 3135
- Power J., Wade G. A., Aurire M., Silvester J. & Hanes D. 2008, *Contrib. Astron. Obs. Skalnate Pleso*, 38, 443
- Roesner W., Wunner G., Herold H., Ruder H., 1984, JPhB, 17, 29
- Ruder H., Wunner G., Herold H., Geyer F., 1994, Atoms in Strong Magnetic Fields. Quantum Mechanical Treatment and Applications in Astrophysics and Quantum Chaos, Springer-Verlag, Heidelberg.
- Schmidt G. D., Smith P. S., 1995, ApJ, 448, 305
- Sion E. M., Fritz M. L., McMullin J. P., Lallo M. D., 1988, AJ, 96, 251
- Tout C.-A., Regos B., 1995, ASPC, 85, 477
- Tout C. A., Wickramasinghe D. T., Ferrario L., 2004, MNRAS, 355, L13
- Tout C. A., Wickramasinghe D. T., Liebert J., Ferrario L., Pringle J. E., 2008, MNRAS, 387, 897
- Tremblay P.-E., Bergeron P., Kalirai J. S., Gianninas A., 2010, ApJ, 712, 1345
- Tremblay P.-E., Bergeron P., Gianninas A., 2011, ApJ, 730, 128
- Tremblay P.-E., Ludwig H.-G., Steffen M., Bergeron P., Freytag B., 2011, A&A, 531, L19
- Zorotovic M., Schreiber M. R., Gänsicke B. T., 2011, A&A, 536, A42
- Wegg C., Phinney E. S., 2012, MNRAS, 426, 427
- Wickramasinghe D. T., Ferrario L., 1988, ApJ, 327, 222
- Wickramasinghe D. T., Ferrario L. 2005, MNRAS, 356, 1576

Name (SDSS J)	P-M-F	$B_{H\alpha}$ (MG)	$B_{H\beta}$ (MG)	S/N	g (mag)	$T_{\text{eff}}$ (K)	$\sigma_T$ (K)	$\log g$ (cgs)	$\sigma_g$ (cgs)
135141.13+541947.35	1323-52797-293	773	K	37.71	16.40	10180	0084	09.64	0.26
234605.44+385337.69	1883-53271-272	706	K	17.74	18.89	99999	0794	05.00	0.01
100356.32+053825.59	0996-52641-295	668	K	15.28	18.11	14019	0140	09.98	0.03
120609.83+081323.72	1623-53089-573	312	K	09.34	19.03	10735	0247	07.65	0.38
221828.59-000012.21	0374-51791-583	212	K	17.30	18.13	12239	0443	09.73	0.24
021148.22+211548.19	2046-53327-048	105	K	36.09	16.73	12986	0134	09.99	0.06
085649.68+253441.07	1933-53381-151	90	-	28.44	17.51	10815	0200	09.91	0.10
080743.33+393829.18	0545-52202-009	65	K	04.07	20.14	10783	0418	08.93	0.67
170400.01+321328.66	0976-52413-319	56	K	04.07	20.42	25597	1118	09.39	0.21
023609.38-080823.91	0455-51909-474	54	-	06.47	19.75	08733	0145	09.93	0.08
114006.37+611008.21	0776-52319-042	53	K	06.41	19.67	10540	0326	09.45	0.45
224741.46+145638.76	0740-52263-444	47	K	29.37	17.39	14771	0069	10.00	0.01
214930.74-072811.97	0644-52173-350	45	K	31.93	17.41	72000	1337	10.00	0.01
121635.36-002656.22	0288-52000-276	45	K	06.51	19.58	11150	0286	09.70	0.26
160357.93+140929.97	2524-54568-247	43	-	16.91	18.29	10123	0055	09.26	0.44
101805.04+011123.52	0503-51999-244	40	K	49.54	16.31	10108	0043	09.87	0.11
094235.02+205208.32	2292-53713-019	38	K	14.39	18.44	13277	0140	09.99	0.02
160437.36+490809.18	0622-52054-330	38	K	20.94	17.90	10084	0012	09.25	0.60
125416.01+561204.67	1318-52781-299	37	K	08.59	19.01	10338	0172	08.62	0.53
151415.66+074446.50	1817-53851-534	36	K	14.92	18.84	10090	0024	09.55	0.38
082835.82+293448.69	1207-52672-635	35	K	06.17	19.74	13176	0327	09.88	0.13
114828.99+482731.23	1446-53080-324	33	K	17.05	18.16	89520	5406	10.00	0.01
075819.57+354443.70	0757-52238-144	32	K	22.10	18.20	12930	0100	10.00	0.01
080938.10+373053.81	0758-52253-044	31	K	10.33	19.01	11398	0320	09.56	0.29
142703.35+372110.51	1381-53089-182	30	34	23.95	17.55	49950	0990	10.00	0.01
172329.14+540755.82	0359-51821-415	30	K	10.13	18.80	10157	0092	09.15	0.50
085153.79+152724.94	2431-53818-238	29	32	08.38	19.42	11300	0388	09.58	0.31
080440.35+182731.03	2081-53357-442	29	K	18.23	18.11	10135	0063	08.46	0.39
011423.35+160727.51	2825-54439-548	28	29	16.90	19.50	46537	1332	10.00	0.01
080359.94+122944.02	2265-53674-033	27	K	31.03	17.27	12347	0109	09.99	0.02
172932.48+563204.09	0358-51818-239	27	K	05.56	20.03	10277	0182	09.18	0.62
115418.14+011711.41	0515-52051-126	26	K	19.69	17.75	79747	3659	10.00	0.01
093415.97+294500.43	2914-54533-162	25	32	25.07	18.95	61840	1821	10.00	0.01
122401.48+415551.91	1452-53112-181	25	K	12.32	18.94	10100	0034	09.35	0.46
113839.51-014903.00	0327-52294-583	24	K	28.51	17.61	10198	0095	09.47	0.31
215148.31+125525.49	0733-52207-522	22	K	20.11	18.10	43262	1151	09.99	0.02
232248.22+003900.88	0383-51818-421	22	K	08.90	19.12	13458	0190	09.97	0.04
023420.63+264801.71	2399-53764-559	21	K	28.75	18.39	57403	0981	10.00	0.01
105628.49+652313.45	0490-51929-205	21	K	09.28	19.71	43262	1894	09.99	0.02
125553.39+152555.08	1771-53498-343	20	2	06.74	19.52	15263	0536	07.68	0.16
125044.43+154957.36*	1770-53171-530	20	K	16.23	18.28	10082	0010	09.66	0.35
125715.54+341439.38	2006-53476-332	19	19	36.15	16.80	38124	0288	10.00	0.01
091124.68+420255.85	1200-52668-538	19	K	13.77	18.84	10108	0043	09.51	0.36
120150.13+614256.93	0778-54525-280	19	17	14.68	18.48	08122	0076	10.00	0.01
	0778-52337-264	8	K	13.50					
105404.38+593333.34	0561-52295-008	18	K	03.51	20.27	09313	0382	09.93	0.08
084201.42+153941.89	2429-53799-363	17	17	06.90	19.73	22510	0794	10.00	0.01
032628.17+052136.35	2339-53729-515	17	K	17.94	18.95	55082	1926	09.99	0.01
225726.05+075541.71	2310-53710-420	17	K	34.35	17.10	85279	2742	09.99	0.02
094458.92+453901.15	1202-52672-577	17	K	05.79	19.92	18919	1136	10.00	0.01
122209.43+001534.06	2568-54153-471	16	K	08.33	20.26	21070	0749	10.00	0.01
	0289-51990-349	16	K	03.23					
053317.32-004321.91	2072-53430-096	16	11	17.06	00.00	71388	5460	07.10	0.24
153829.29+530604.65	0795-52378-637	16	K	08.51	19.26	18116	0547	10.00	0.01

Name (SDSS J)	P-M-F	$B_{H\alpha}$ (MG)	$B_{H\beta}$ (MG)	S/N	g (mag)	$T_{\text{eff}}$ (K)	$\sigma_T$ (K)	$\log g$ (cgs)	$\sigma_g$ (cgs)
131508.97+093713.87	1798-53851-233	14	-	45.27	16.23	72414	1249	10.00	0.01
074924.91+171355.45	2729-54419-282	14	K	22.57	18.78	35795	0432	10.00	0.01
072540.82+321402.12	2695-54409-564	14	13	07.43	20.06	34711	1100	09.99	0.02
100759.81+162349.64	2585-54097-030	14	K	22.19	17.74	32642	0275	10.00	0.01
083448.65+821059.00	2549-54523-135	14	K	28.14	18.33	41210	0539	10.00	0.01
134820.80+381017.25	2014-53460-236	14	K	23.58	17.55	45528	0864	10.00	0.01
133340.34+640627.38	0603-52056-112	14	K	19.01	17.88	20048	0152	10.00	0.01
115345.97+133106.61	1762-53415-042	13	-	05.56	19.81	12844	0540	09.19	0.40
143235.46+454852.52	2932-54595-542	13	K	09.68	19.94	21053	0492	09.99	0.02
101428.10+365724.40	1954-53357-393	13	13	12.95	18.85	19580	0342	10.00	0.01
140716.67+495613.70	1671-53446-453	13	K	09.49	19.14	27376	0610	10.00	0.01
101428.10+365724.40	1426-52993-021	13	13	08.49	18.85	17225	0724	09.99	0.02
205233.52-001610.69	0982-52466-019	13	K	12.40	18.51	36761	0831	09.99	0.01
074947.00+354055.51	0542-51993-639	13	12	11.00	19.75	39100	1213	09.98	0.03
152401.60+185659.21	2794-54537-410	12	K	20.77	18.16	22067	0290	10.00	0.01
085550.68+824905.20	2549-54523-066	12	K	22.40	18.64	32081	0265	10.00	0.01
103350.88+204729.40	2376-53770-463	12	13	08.00	19.42	34544	0947	09.98	0.03
090748.82+353821.5	1212-52703-187	12	K	-	19.61	12485	0306	09.85	0.14
001034.95+245131.20	2822-54389-025	11	11	10.43	19.84	19355	0654	10.00	0.01
075234.95+172524.86	2729-54419-171	11	11	28.79	18.46	39779	0471	10.00	0.01
	1920-53314-106	12	K	17.67					
202501.11+131025.62	2257-53612-167	11	K	23.72	18.77	28932	0199	10.00	0.01
120547.48+340811.48	2089-53498-431	11	12	09.00	19.63	23237	0632	10.00	0.01
033145.69+004517.04	0810-52672-391	11	11	45.85	17.20	28299	0095	10.00	0.01
	2049-53350-450	11	11	33.80					
	0415-51879-378	12	13	32.22					
	0415-51810-370	12	K	32.86					
081648.71+041223.53	1184-52641-329	11	10	03.44	20.39	12880	0912	09.95	0.06
030407.40-002541.74	0709-52205-120	11	11	26.97	17.75	21828	0227	10.00	0.01
	2048-53378-280	10	10	26.18					
	0411-51817-172	11	10	23.40					
	0411-51873-172	19	18	22.83					
	0710-52203-311	11	11	21.25					
115917.39+613914.32	0777-52320-069	10	K	07.64	18.97	35770	1193	09.99	0.02
121209.31+013627.72	0518-52282-285	10	K	21.90	18.00	24706	0182	10.00	0.01
031824.20+422651.00	2417-53766-568	9.9	9.2	30.87	18.21	20274	0098	10.00	0.01
084008.50+271242.70	1587-52964-059	9.8	10	08.06	19.17	19113	0355	09.99	0.02
172045.37+561214.90	0367-51997-461	9.7	K	06.24	20.10	46580	3487	09.95	0.06
153843.11+084238.27	1725-54266-297	9.6	K	19.58	17.92	33803	0340	09.99	0.01
165203.68+352815.81	0820-52438-299	9.5	K	09.99	19.23	18778	0406	09.94	0.07
034308.18-064127.35	0462-51909-117	9.2	K	08.82	19.48	11718	0447	09.57	0.32
153532.25+421305.62	1052-52466-252	9.1	K	03.21	20.37	18143	1006	08.10	0.24
091437.35+054453.31	1193-52652-481	8.9	K	28.18	17.33	23420	0229	10.00	0.01
123204.20+522548.27	0885-52379-319	8.9	9.6	10.25	18.82	08183	0093	09.29	0.10
124851.31-022924.73	2922-54612-607	8.8	8.7	34.75	18.42	19835	0070	10.00	0.01
112030.34-115051.14	2874-54561-512	8.8	8.7	21.88	18.73	27302	0222	10.00	0.01
093126.14+321946.15	1943-53386-294	8.6	8.3	07.49	19.23	16248	0629	09.58	0.12
122249.14+481133.14	1451-53117-582	8.6	8.3	13.72	18.72	09790	0093	10.00	0.01
151130.17+422023.00	1291-52735-612	8.4	K	19.79	17.99	30882	0265	10.00	0.01
	1291-52738-615	12	12	18.41					
154213.48+034800.43	0594-52045-400	8.2	K	11.35	19.12	15760	0877	10.00	0.01
113756.50+574022.43	1311-52765-421	8.1	8.3	29.48	16.87	10080	0002	09.03	0.80

Name (SDSS J)	P-M-F	$B_{H\alpha}$ (MG)	$B_{H\beta}$ (MG)	S/N	g (mag)	$T_{\text{eff}}$ (K)	$\sigma_T$ (K)	$\log g$ (cgs)	$\sigma_g$ (cgs)
100005.67+015859.18	0500-51994-557	8.1	K	05.03	20.04	08124	0141	09.96	0.05
171441.08+552711.45	0367-51997-318	8.1	9.2	06.27	20.23	36207	1509	07.45	0.25
150813.25+394504.91	1398-53146-633	8.0	K	28.17	17.89	29032	0167	09.52	0.04
074853.08+302543.56	0889-52663-507	8.0	K	34.70	17.59	28932	0116	09.73	0.04
124851.31-022924.69	0337-51997-264	8.0	K	12.17	18.42	18000	0212	09.59	0.05
085523.87+164059.01	2431-53818-522	7.9	K	12.84	18.56	28315	0477	10.00	0.01
023445.31+260553.18	2399-53764-487	7.8	7.4	05.59	20.72	19105	0558	09.94	0.07
113357.66+515204.85	0879-52365-586	7.7	K	29.49	17.33	24938	0173	10.00	0.01
112257.11+322327.80	1979-53431-512	7.5	K	08.49	19.37	18771	0482	10.00	0.01
101618.37+040920.58	0574-52355-166	7.2	K	03.47	20.29	12275	0732	09.93	0.07
130033.48+590407.05	2461-54570-015	6.8	6.5	26.57	18.23	06300	0004	10.00	0.01
014230.57+003502.66	1907-53315-427	6.6	5.7	09.96	19.99	10676	0131	07.90	0.13
	1907-53265-425	1.7	-	09.96					
080502.29+215320.54	1584-52943-132	6.6	7.0	18.52	18.61	37141	0575	09.39	0.07
083438.29+153817.48	2427-53815-321	6.5	5.7	03.40	20.24	12290	0569	08.27	0.24
122748.85+385546.34	1986-53475-090	6.5	7.0	06.24	19.49	18116	0554	09.81	0.12
143019.06+281100.87	2134-53876-423	6.2	K	24.73	17.68	07906	0053	09.48	0.04
111010.50+600141.44	2414-54526-323	6.1	6.5	31.79	17.99	35974	0282	09.57	0.04
	0950-52378-568	6.7	K	17.38					
151745.19+610543.59	0613-52345-446	6.1	K	03.68	20.52	13748	1001	09.92	0.09
231951.73+010909.32	0382-51816-565	6.1	K	14.00	18.51	07525	0062	09.02	0.11
170916.37+234111.33	1688-53462-508	6.0	-	04.04	20.29	17102	0998	09.62	0.17
090632.66+080715.96	1300-52973-148	6.0	K	17.54	18.66	46580	1335	09.93	0.07
102220.70+272539.85	2350-53765-543	5.8	K	05.32	20.06	14780	0667	09.12	0.17
165249.09+333444.90	1175-52791-095	5.8	K	09.89	18.64	09593	0102	09.32	0.10
171831.24+280825.72	0980-52431-434	5.6	-	05.35	19.87	44249	3458	07.15	0.46
153315.26+564200.32	0614-53437-579	5.6	6.1	04.20	20.39	08017	0164	09.63	0.28
144614.00+590216.73	0608-52081-140	5.6	7.0	04.47	20.11	15794	0569	09.11	0.17
100657.52+303338.10	1953-53358-415	5.5	4.8	11.90	18.82	14462	0303	08.94	0.08
215248.44-010324.17	1107-52968-374	5.5	K	04.67	20.29	08990	0208	08.20	0.35
111150.80+663736.20	0490-51929-639	-	5.4	05.23	20.05	18084	0681	07.59	0.16
014313.18+231524.60	2064-53341-024	5.3	-	04.40	20.73	43788	3957	08.91	0.49
134043.10+654349.20	0497-51989-182	5.3	K	15.47	18.47	19819	0249	09.99	0.02
134043.11+654349.26	2460-54616-013	5.1	5.2	22.77	18.47	18612	0179	09.51	0.03
083627.35+154850.31	2276-53712-107	5.1	7.0	09.49	19.28	47547	2422	08.84	0.22
013533.19+132249.90	0426-51882-291	5.0	5.2	02.14	20.46	13480	1164	08.70	0.37
125434.65+371000.19	1989-53772-041	4.9	K	46.84	16.01	25365	0140	09.27	0.02
053126.76+001738.13	2072-53430-427	4.6	3.5	05.35	20.69	17753	0907	07.70	0.17
012339.94+405241.88	2063-53359-403	4.6	3.5	06.41	20.27	36761	1448	07.48	0.22
120806.26+144942.97	1764-53467-112	4.6	2.5	04.03	20.16	11691	0507	08.27	0.26
144934.73+025502.62	0537-52027-566	4.6	4.4	09.86	18.98	07961	0097	09.36	0.16
144408.76+024327.75	0537-52027-371	4.6	3.9	06.58	19.45	10129	0063	09.22	0.54
075816.64+121428.68	2265-53674-199	4.5	3.9	09.47	19.00	13625	0354	08.39	0.09

Name (SDSS J)	P-M-F	$B_{H\alpha}$ (MG)	$B_{H\beta}$ (MG)	S/N	g (mag)	$T_{\text{eff}}$ (K)	$\sigma_T$ (K)	$\log g$ (cgs)	$\sigma_g$ (cgs)
064828.76+840340.87	2548-54152-616	4.3	4.4	11.34	19.75	17290	0320	09.24	0.07
102535.40+282034.79	2351-53772-007	4.3	3.9	07.47	19.74	24023	0790	07.85	0.14
090522.06+205736.32	2284-53708-091	4.3	4.8	08.34	19.36	12469	0389	08.17	0.14
004528.87+004616.44	1905-53706-526	4.3	3.0	16.40	19.26	17439	1340	09.27	0.07
153057.50+394615.03	1293-52765-613	4.3	-	03.45	20.38	15575	0794	07.32	0.22
093447.90+503312.19	0901-52641-373	4.3	K	10.97	18.82	08946	0098	09.99	0.01
105328.14+505155.14	0876-52669-510	4.3	4.4	06.01	19.87	09055	0148	09.07	0.20
003111.75+134919.53	0417-51821-084	4.3	4.8	03.14	20.21	16953	1101	08.49	0.22
031323.65-001659.86	0413-51929-313	4.3	4.4	06.26	19.79	65455	8331	08.68	0.56
101339.47+352639.61	1954-53357-250	4.2	1.5	05.20	20.02	16128	0547	07.53	0.15
124836.32+294231.26	2457-54180-112	4.0	K	25.85	17.82	06489	0020	10.00	0.01
084510.23+112405.61	2428-53801-089	4.0	4.8	04.07	20.01	13659	1059	07.22	0.25
152203.45+203438.96	2156-54525-031	4.0	3.9	11.06	18.79	19850	0453	07.85	0.08
124816.82+411051.23	1985-53431-445	4.0	3.5	09.71	19.14	20265	0440	09.49	0.08
154305.67+343223.68	1402-52872-145	4.0	K	13.55	18.33	30620	0335	09.24	0.07
091314.46+410838.75	1200-52668-079	4.0	2.0	04.47	20.20	12110	0599	08.37	0.20
144345.84+482008.97	1047-52733-099	4.0	4.0	05.00	19.75	16811	0606	07.43	0.16
085130.57+353117.59	0934-52672-080	4.0	4.0	04.99	19.79	07581	0119	08.98	0.50
104356.64+650057.24	0489-51930-079	4.0	3.9	05.26	20.03	12488	0399	07.84	0.19
091611.08+124808.09	2577-54086-427	3.9	3.9	06.15	19.89	15711	0465	07.78	0.12
102239.06+194904.33	2374-53765-544	3.9	3.5	11.42	19.02	10060	0096	09.42	0.08
165029.91+341125.50	1175-52791-482	3.9	K	11.26	18.77	11921	0186	09.25	0.09
121110.30+203429.05	2609-54476-564	3.8	3.0	08.72	19.77	23497	0635	07.78	0.10
114917.23+300016.08	2222-53799-593	3.8	3.5	15.53	18.77	09927	0066	08.69	0.07
224742.58-003317.39	0676-52178-319	3.8	4.4	05.52	19.63	57600	7109	07.21	0.62
132203.94+193223.08	2619-54506-423	3.6	2.2	04.61	20.30	11413	0351	07.91	0.20
093726.27+205756.98	2361-53762-408	3.6	3.5	05.25	19.99	12266	0522	08.14	0.20
092355.98+243552.86	2291-53714-552	3.6	3.9	03.99	20.41	12976	0662	08.57	0.21
113048.38+305720.74	1974-53430-222	3.6	3.9	07.09	19.65	12647	0425	09.66	0.15
211125.84+110219.69	1890-53237-390	3.6	3.5	25.85	17.40	18577	0123	09.45	0.02
235431.38+365019.13	1881-53261-512	3.6	3.5	06.44	20.48	14078	1251	09.29	0.17
124806.38+410427.15	1456-53115-190	3.6	K	19.35	17.90	06574	0032	10.00	0.01
120728.96+440731.62	1369-53089-048	3.6	3.8	06.87	19.32	18813	0520	07.97	0.12
094711.11+003754.69	0480-51989-082	3.6	4.4	07.56	19.74	13827	3547	08.11	0.33
081136.34+461156.44	0439-51877-523	3.6	4.8	06.29	19.82	27097	1515	07.20	0.37
081523.35+084346.43	2571-54055-256	3.5	3.5	04.16	20.27	13816	0655	08.11	0.20
203256.48+142651.99	2258-54328-278	3.5	2.6	07.85	20.57	19968	0886	07.92	0.16
114833.25+303921.27	2222-53799-577	3.5	3.5	04.71	20.23	11053	0301	08.62	0.17
090937.95+250820.64	2086-53401-582	3.5	3.7	09.80	19.01	11012	0154	08.80	0.09

Name (SDSS J)	P-M-F	$B_{H\alpha}$ (MG)	$B_{H\beta}$ (MG)	S/N	g (mag)	$T_{\text{eff}}$ (K)	$\sigma_T$ (K)	$\log g$ (cgs)	$\sigma_g$ (cgs)
153301.50+550840.72	0614-53437-079	3.5	2.6	05.72	19.94	09644	0153	08.23	0.24
154135.02+030051.14	0594-52045-253	3.5	4.4	04.15	20.33	11024	0366	09.18	0.26
010225.14-005458.15	0693-52254-099	-	3.5	07.95	19.26	18564	1798	09.00	0.14
081716.39+200834.89	2082-53358-444	3.4	K	16.66	18.35	06886	0043	09.99	0.02
011130.67+141049.67	2825-54439-089	3.3	3.0	06.99	19.97	15022	0784	07.91	0.13
091340.19+114112.41	2576-54086-029	3.3	3.9	06.80	19.54	15422	0486	07.76	0.12
212329.46-081004.44	2320-54653-090	3.3	3.0	08.36	19.98	16056	0373	08.88	0.10
131544.04+262333.30	2243-53794-170	3.3	3.0	06.30	19.69	09008	0151	09.26	0.17
163600.25+354625.33	2185-53532-320	3.3	3.9	18.32	19.21	24080	0368	07.99	0.05
083918.12+212143.79	2084-53360-100	3.3	3.9	04.11	20.10	10813	0394	09.82	0.15
083041.78+204233.84	2083-53359-553	3.3	3.5	07.92	19.39	16175	0467	08.37	0.09
125101.98+351913.59	1987-53765-570	3.3	2.6	09.07	19.07	19827	0413	08.34	0.09
074403.81+495440.02	1868-53318-410	3.3	1.5	14.08	18.75	36390	0736	09.65	0.12
161047.77+235301.87	1852-53534-567	3.3	2.6	04.95	19.83	09365	0167	09.95	0.06
114827.96+153356.97	1762-53415-372	3.3	3.0	04.97	20.17	11515	0418	09.07	0.16
155436.25+413956.61	1334-52764-235	3.3	-	03.69	20.12	19749	0960	09.24	0.22
110735.32+085924.59	1221-52751-177	3.3	3.5	13.05	18.43	18997	0344	09.15	0.06
082533.22+412400.15	0760-52264-640	3.3	3.5	05.43	19.79	16149	0590	07.78	0.14
224103.30+132853.25	0739-52520-143	3.3	3.5	05.76	19.78	22940	0856	07.36	0.19
094815.27+041648.67	0570-52266-632	3.3	3.5	04.44	19.75	12311	0704	07.64	0.23
095211.45+563020.74	0557-52253-170	3.3	3.5	11.81	18.69	22652	0509	07.98	0.08
084937.77+561949.27	0483-51902-296	3.3	4.4	05.27	20.11	10008	0195	09.04	0.25
094012.89-000009.88	0476-52314-597	3.3	2.6	05.98	19.63	22232	0843	08.07	0.14
094046.29+595415.92	0453-51915-325	3.3	3.0	07.05	19.57	10769	0228	07.83	0.17
121105.25-004628.45	0287-52023-253	3.3	4.4	13.99	18.69	22490	0371	09.06	0.06
115817.44+331719.26	2095-53474-337	3.2	2.6	05.15	19.80	19976	0697	08.31	0.15
115554.95+083549.54	1622-53385-447	3.2	2.6	12.38	18.88	09888	0089	09.37	0.07
120125.40+084800.44	1228-52728-220	3.2	-	09.39	18.68	06965	0064	09.99	0.02
095738.55+194601.95	2363-53763-097	3.1	3.5	04.01	20.21	13411	0760	09.44	0.24
230758.83+000500.32	0678-52884-498	3.1	3.4	05.12	20.04	13923	1877	08.02	0.30
145801.10+040917.03	0588-52029-639	3.1	3.5	03.97	19.90	08729	0133	05.15	0.15
092527.47+011328.66	0475-51965-315	3.1	K	12.04	18.60	11016	0104	09.01	0.10
032137.44+010437.38	0413-51821-578	3.1	3.5	03.76	19.92	13729	1414	08.07	0.23
025837.20+000019.27	0410-51877-065	3.1	4.4	05.38	19.73	11053	0688	08.47	0.21
154141.85+173026.25	2795-54563-603	3.0	2.2	06.13	19.86	14074	0605	07.95	0.14
121211.28+185228.97	2609-54476-005	3.0	3.0	06.73	19.92	20758	0675	08.10	0.13
103002.67+163927.45	2592-54178-417	3.0	2.6	04.68	20.09	18334	0747	07.99	0.17
083310.57+234812.72	2330-53738-109	3.0	2.2	06.08	20.48	11111	0250	08.80	0.21
012115.45+321010.04	2061-53711-506	3	5.0	06.88	20.36	17585	0583	08.03	0.12
131050.04+143520.47	1772-53089-559	3.0	-	05.23	19.74	69903	1018	7.91	0.58
151102.75+433558.73	1677-53148-151	3.0	2.6	04.19	20.36	09472	0194	08.02	0.30
093409.91+392759.33	1215-52725-241	3.0	2.6	15.62	18.35	10985	0091	09.03	0.07
105216.00+530120.32	1010-52649-597	3.0	-	04.78	20.25	12698	0633	07.98	0.20
100822.39+015307.46	0501-52235-077	3.0	3.8	08.31	19.50	57534	6042	07.27	0.39
090343.14+011846.39	0470-51929-403	3.0	2.1	06.34	19.62	07930	0090	05.10	0.11

Name (SDSS J)	P-M-F	$B_{H\alpha}$ (MG)	$B_{H\beta}$ (MG)	S/N	g (mag)	$T_{\text{eff}}$ (K)	$\sigma_T$ (K)	$\log g$ (cgs)	$\sigma_g$ (cgs)
084155.74+022350.56	0564-52224-248	2.9	K	16.21	18.99	06587	0038	10.00	0.01
161929.63+131833.45	2530-53881-332	2.8	2.6	05.73	19.70	16471	0554	07.74	0.15
091305.88+173932.93	2439-53795-357	2.8	3.0	05.56	19.80	12792	0565	07.88	0.16
114529.27+300824.36	2222-53799-483	2.8	3.0	07.75	19.62	19811	0483	07.77	0.14
113215.39+280934.31	2219-53816-329	2.8	K	29.39	17.02	06896	0029	10.00	0.01
161147.94+211136.64	2205-53793-542	2.8	3.5	06.96	20.05	10303	0190	07.97	0.17
154856.94+230727.92	2169-53556-491	2.8	2.6	13.73	18.73	09732	0075	08.62	0.09
012105.53+393239.65	2062-53381-337	2.8	3.0	10.67	19.67	21640	0511	07.99	0.08
235318.57+380913.17	1883-53271-050	2.8	1.0	10.54	19.44	13142	0679	09.48	0.09
153554.18+404414.16	1679-53149-109	2.8	1.7	04.31	20.27	21818	1067	07.72	0.21
125040.82+590341.61	2461-54570-219	2.7	2.6	05.50	20.01	22340	0802	09.00	0.16
011739.82+242236.26	2060-53706-086	2.7	2.0	10.36	19.54	14558	0391	07.80	0.09
112014.62+400422.61	1980-53433-630	2.7	2.0	08.99	19.50	13214	0461	09.00	0.10
101834.81+303330.46	1956-53437-197	2.7	-	05.75	19.78	30657	0876	09.97	0.04
100715.55+123709.51	1745-53061-313	2.7	4.0	09.27	18.76	19772	0388	09.69	0.08
143308.50+102623.05	1709-53533-511	2.7	1.5	17.07	18.28	06657	0033	10.00	0.01
010214.99+462620.93	1472-52913-278	2.7	1.5	12.20	00.00	08033	0068	07.42	0.17
111812.67+095241.36	1222-52763-477	2.7	K	10.86	18.75	14306	0333	08.90	0.08
084910.13+044528.71	1188-52650-635	2.7	1.6	08.11	19.29	09959	0155	05.99	0.18
220524.61+010503.35	1105-52937-404	2.7	2.5	09.07	19.46	16385	0511	09.19	0.08
095919.86+573542.89	0558-52317-158	2.7	2.6	03.88	20.27	12278	1478	07.93	0.47
151436.66+152058.48	2766-54242-497	2.6	3.0	14.98	18.53	11318	0104	09.25	0.06
225338.68+301803.47	2627-54379-021	2.6	2.2	05.44	19.86	16930	0512	08.32	0.13
161050.03+094302.45	2526-54582-115	2.6	2.6	04.88	19.97	25289	1193	07.78	0.19
160219.42+112606.53	2525-54569-303	2.6	2.6	05.62	19.85	09800	0151	08.27	0.20
030432.89+365537.88	2443-54082-137	2.6	2.6	05.07	20.83	19718	1180	07.73	0.21
084219.70+122128.36	2428-53801-221	2.6	2.6	04.79	19.74	11929	0765	07.74	0.22
103532.53+212603.56	2376-53770-534	2.6	2.7	23.44	17.40	06763	0031	09.99	0.02
092041.54+221545.53	2319-53763-557	2.6	2.6	06.73	20.35	17734	0574	07.99	0.12
080210.39+153033.83	2266-53679-534	2.6	2.2	08.79	19.79	11364	0205	08.07	0.12
151606.35+274647.04	2154-54539-637	2.6	3.0	14.23	18.38	41076	1071	07.94	0.11
141906.20+254356.51	2131-53819-317	2.6	K	26.50	17.41	09906	0033	08.62	0.04
074958.59+161120.32	2080-53350-349	2.6	2.6	04.28	20.25	14499	0638	07.54	0.17
073953.18+204900.26	2079-53379-051	2.6	3.0	08.80	19.92	15385	0413	07.78	0.09
013909.15+230845.00	2064-53341-163	2.6	-	05.03	20.69	19303	0850	08.12	0.18
121529.85+335158.62	1999-53503-238	2.6	2.8	08.68	19.17	17847	0373	08.07	0.09
135654.77+343617.25	1838-53467-240	2.6	2.0	06.95	19.91	34146	0949	07.82	0.19
132002.48+131901.57	1773-53112-011	2.6	K	06.72	19.50	15204	0449	07.87	0.11
081144.60+071030.58	1756-53080-585	2.6	2.6	08.64	19.41	17470	0375	07.64	0.10
170019.42+245701.18	1693-53446-169	2.6	2.0	04.44	20.00	29422	0996	07.89	0.21
134017.71+594552.42	0786-52319-254	2.6	3.0	12.17	19.03	35770	0685	07.57	0.12
032300.93+002221.32	0712-52199-427	2.6	2.6	03.93	20.43	11906	1209	07.51	0.35
004248.19+001955.26	0690-52261-594	2.6	K	08.16	19.52	10398	0135	09.98	0.03
233328.30-002036.70	0682-52525-317	2.6	2.7	05.05	19.98	08401	0169	08.18	0.31
225230.63+003232.68	0676-52178-481	2.6	3.0	06.21	19.65	61017	6944	08.14	0.38
204626.15-071036.98	0635-52145-227	2.6	K	20.70	17.95	09385	0049	09.19	0.06
220823.66-011534.05	0373-51788-086	2.6	2.3	14.46	21.75	29770	0369	07.36	0.08
161425.46+493244.91	2884-54526-254	2.5	3.0	07.64	19.64	13744	0570	07.44	0.12
100645.00+144250.28	2586-54169-479	2.5	2.6	08.48	19.64	11436	0247	07.95	0.13
082939.25+100937.73	2572-54056-399	2.5	2.2	08.13	19.72	15613	0489	08.15	0.09
085106.13+120157.84	2430-53815-229	2.5	K	28.17	16.98	14078	0110	08.45	0.03
091833.32+205536.97	2319-53763-209	2.5	2.6	22.03	18.41	15584	0173	08.46	0.03
	2290-53727-247	2.3	2.4	16.41					
	2288-53699-547	2.7	-	13.15					
080638.51+075647.55	2076-53442-521	2.5	2.6	09.66	19.98	15580	0409	07.92	0.09

Name (SDSS J)	P-M-F	$B_{H\alpha}$ (MG)	$B_{H\beta}$ (MG)	S/N	g (mag)	$T_{\text{eff}}$ (K)	$\sigma_T$ (K)	$\log g$ (cgs)	$\sigma_g$ (cgs)
073001.65+362713.10	2073-53728-482	2.5	2.6	10.17	19.65	13877	0554	08.13	0.09
103935.51+295413.59	1969-53383-215	2.5	3.0	12.77	18.62	14388	0357	09.08	0.07
235503.84+350659.75	1881-53261-042	2.5	2.2	08.17	19.51	28094	0767	07.78	0.15
073741.50+470421.09	1867-53317-457	2.5	2.6	13.61	18.83	56439	2781	07.65	0.19
133828.43+415943.85	1464-53091-605	2.5	3.5	09.93	18.92	09270	0094	09.95	0.06
093356.40+102215.69	1303-53050-525	2.5	K	11.68	18.77	09075	0082	08.81	0.10
104113.70+083505.23	1240-52734-105	2.5	-	04.81	19.84	62299	8856	09.82	0.18
081130.21+305720.54	0861-52318-096	2.5	3.5	07.35	19.63	08045	0101	09.87	0.13
105709.82+041130.37	0580-52368-274	2.5	K	23.80	17.70	07287	0035	08.65	0.05
034511.11+003444.27	0416-51811-590	2.5	2.6	16.89	18.65	07157	0065	09.30	0.12
220435.05+001242.95	0372-52173-626	2.5	K	06.11	19.35	10426	0183	08.98	0.22
173915.64+545059.26	0360-51816-547	2.5	2.2	05.27	19.84	12104	0799	07.70	0.23
083420.29+131759.52	2426-53795-387	2.4	3.5	05.05	19.84	14114	0644	08.01	0.15
123414.11+124829.58	1616-53169-423	2.4	K	26.06	17.39	08544	0049	09.27	0.04
164357.02+240201.31	1414-53135-191	2.4	K	07.44	19.24	18715	0521	07.99	0.10
112926.23+493931.86	0966-52642-474	2.4	K	20.09	18.02	20160	0210	09.33	0.04
093921.25+581421.45	0452-51911-553	2.4	3.0	04.62	20.02	12776	0447	05.17	0.15
154524.79+010127.54	2955-54562-061	2.3	2.2	04.38	19.92	13074	1045	07.81	0.23
064532.74+280330.46	2694-54199-201	2.3	3.0	10.29	19.75	11351	1245	08.33	0.19
122100.20+244443.75	2657-54502-026	2.3	2.2	09.03	19.28	11165	0176	07.81	0.12
173208.55+631950.33	2561-54597-087	2.3	2.2	09.15	20.05	16082	0457	08.02	0.10
090907.15+193840.65	2286-53700-176	2.3	2.6	05.22	19.99	09871	0176	08.04	0.20
205000.94+170145.59	2259-53565-530	2.3	2.6	08.24	19.80	15167	0388	07.98	0.09
113055.05+260115.62	2218-53816-081	2.3	2.6	05.01	20.07	15493	0576	07.82	0.16
141813.22+312340.13	2129-54243-426	2.3	2.2	09.39	19.13	07507	0076	09.90	0.10
	2129-54252-426	2.3	2.2	09.39					
091305.58+260748.62	2087-53415-383	2.3	2.6	04.01	20.28	12200	0520	08.17	0.20
013314.21+235247.30	2064-53341-343	2.3	-	11.09	19.58	99018	3502	05.25	0.94
120924.84+331716.41	2004-53737-418	2.3	-	10.62	19.33	06582	0059	09.90	0.12
081632.26+522645.27	1781-53297-148	2.3	1.5	08.27	19.29	07051	0085	09.50	0.23
164626.65+222645.45	1570-53149-615	2.3	2.2	09.31	19.15	14991	0441	08.40	0.08
114852.78+430753.14	1447-53120-323	2.3	-	06.03	19.69	53961	5373	07.74	0.42
091220.26+075537.71	1301-52976-241	2.3	3.0	05.05	20.20	12920	0556	09.26	0.16
082239.55+304857.26	0931-52619-078	2.3	2.0	04.64	20.33	14347	0666	06.48	0.21
030417.84-003216.31	0709-52205-107	2.3	3.0	05.63	19.90	10971	1015	08.09	0.32
094351.26+010104.13	0480-51989-251	2.3	3.5	05.94	20.13	09081	0146	07.81	0.32
092242.42+011422.80	0473-51929-003	2.3	3.0	06.73	19.65	31980	0771	07.72	0.25
034240.64-073504.00	0462-51909-084	2.3	3.5	04.97	20.14	14621	1586	08.03	0.23
021230.01+122557.17	0428-51883-046	2.3	1.7	04.53	20.24	14334	2878	07.62	0.30
013920.55+152218.81	0426-51882-524	2.3	3.3	04.49	19.86	13386	0857	08.49	0.31
231432.88-011320.52	0382-51816-289	2.3	2.6	03.38	20.43	11787	0885	09.69	0.22
112852.88-010540.82	0326-52375-565	2.3	K	03.56	20.38	14189	1254	07.78	0.25
141309.30+191832.01	2772-54529-217	2.2	1.9	21.46	18.20	18625	0186	09.33	0.03
102746.58+435156.30	2567-54179-306	2.2	2.2	08.11	19.73	14462	0452	08.35	0.10
154550.72+132040.19	2517-54567-065	2.2	2.2	08.46	19.32	12682	0501	08.06	0.14
030913.96+373057.90	2443-54082-030	2.2	3.0	04.40	20.83	24115	1662	07.44	0.24
031929.02+410316.92	2417-53766-064	2.2	1.3	07.20	20.20	21275	0844	07.93	0.13
023542.73+241653.78	2399-53764-030	2.2	2.6	08.70	19.90	12472	0515	08.13	0.13
024903.02+332737.09	2398-53768-313	2.2	2.2	08.92	19.82	18495	0502	07.70	0.10
102429.18+281435.40	2351-53786-001	2.2	2.2	10.05	19.09	16884	0345	07.43	0.08
100727.33+281457.81	2348-53757-279	2.2	2.2	05.38	19.83	10783	0242	07.99	0.29
212425.74-064837.14	2320-54653-544	2.2	2.2	13.64	19.51	16822	0399	08.98	0.06
083945.56+200015.76	2277-53705-484	2.2	K	22.28	17.84	17326	0143	09.02	0.03
082817.61+181752.64	2275-53709-298	2.2	2.6	09.03	19.53	13673	0412	08.09	0.09
105833.57+372401.35	2091-53447-464	2.2	2.2	06.76	19.44	11457	0266	08.79	0.14
012815.72+391130.02	2063-53359-063	2.2	2.6	05.16	20.29	15153	0624	07.90	0.14
224707.32+010058.47	1901-53261-564	2.2	2.2	06.72	20.43	20622	0717	08.32	0.14
151625.08+280320.92	1846-54173-280	2.2	2.2	35.41	16.62	06810	0022	10.00	0.00
145415.01+432149.51	1290-52734-469	2.2	K	08.42	19.07	14437	0302	08.62	0.09
101420.38+060254.02	0996-52641-025	2.2	2.0	03.96	19.84	13023	0515	07.56	0.18
085830.85+412635.12	0830-52293-070	2.2	2.2	33.00	17.06	06699	0021	10.00	0.00

Name (SDSS J)	P-M-F	$B_{H\alpha}$ (MG)	$B_{H\beta}$ (MG)	S/N	g (mag)	$T_{\text{eff}}$ (K)	$\sigma_T$ (K)	$\log g$ (cgs)	$\sigma_g$ (cgs)
164703.24+370910.29	0818-52395-026	2.2	K	20.88	17.63	17872	0177	09.00	0.03
234623.69-102357.03	0648-52559-142	2.2	K	14.87	18.43	07447	0048	10.00	0.01
130807.48-010117.05	0294-51986-089	2.2	2.8	09.76	19.13	11699	0253	08.59	0.10
084936.81+224754.97	2085-53379-131	2.1	2.1	05.19	19.72	18694	0659	08.07	0.14
120803.24+625815.33	0778-54525-511	2.1	1.7	06.72	19.76	62454	7120	07.46	0.46
004122.49-110432.49	0655-52162-091	2.1	3.5	07.04	19.26	06977	0077	09.94	0.07
150220.91+001721.08	0539-52017-202	2.1	2.8	03.85	19.86	07601	0175	08.63	0.54
003232.07+153126.55	0418-51817-346	2.1	2.4	05.01	19.77	12616	0597	07.99	0.17
153349.02+005916.15	2954-54561-048	2.0	2.6	16.54	18.18	14920	0181	08.40	0.04
112216.04-122250.99	2874-54561-071	2.0	1.9	07.02	20.42	15259	0887	08.16	0.14
173056.42+433000.41	2820-54599-185	2.0	2.4	05.35	20.29	12993	0616	08.15	0.20
164649.56+120547.10	2817-54627-308	2.0	2.2	13.48	19.13	80899	6363	07.74	0.26
224854.52+303845.57	2627-54379-152	2.0	2.2	06.30	19.85	18855	0677	07.82	0.14
083801.81+092548.30	2573-54061-246	2.0	2.6	05.28	20.16	22540	1028	07.07	0.24
174235.19+640028.36	2561-54597-021	2.0	1.7	05.44	20.37	17004	0832	07.88	0.18
105556.92+483652.49	2410-54087-494	2.0	2.2	07.31	20.31	13559	0781	08.50	0.15
092524.26+175712.64	2360-53728-217	2.0	1.9	10.41	18.80	17314	0309	07.90	0.08
101059.22+284359.73	2348-53757-485	2.0	2.1	04.07	20.33	14512	2382	08.08	0.46
030522.15+050213.33	2322-53727-024	2.0	2.6	07.15	20.20	12591	0513	08.45	0.16
092246.94+230812.74	2319-53763-567	2.0	1.8	06.71	20.33	16993	0521	08.06	0.11
094025.98+201707.30	2292-53713-048	2.0	2.8	06.85	19.55	13666	0819	07.63	0.14
093059.16+202429.35	2289-53708-069	2.0	2.6	07.45	19.90	14229	0739	07.76	0.12
091132.80+223200.66	2287-53705-169	2.0	1.9	07.63	19.63	11146	0210	08.30	0.14
090554.64+213829.62	2284-53708-103	2.0	2.2	07.37	19.52	24597	0708	07.42	0.14
083701.89+154454.66	2276-53712-004	2.0	1.9	09.62	19.17	15980	0329	08.16	0.08
112439.29+262422.76	2216-53795-143	2.0	-	06.48	19.48	13047	0432	07.89	0.14
140051.72+330754.37	2121-54180-369	2.0	1.9	09.40	19.39	22018	0548	07.81	0.09
053507.04+001617.23	2072-53430-508	2.0	3.0	10.11	19.96	23486	0635	08.38	0.09
110203.75+400558.02	1988-53469-434	2.0	3.0	05.79	19.80	09511	0147	09.08	0.16
113804.16+305310.59	1974-53430-023	2.0	2.0	04.88	19.97	11273	0373	09.08	0.27
155818.96+241758.75	1851-53524-476	2.0	2.0	04.35	20.06	13618	0850	09.13	0.20
155657.69+231358.47	1851-53524-298	2.0	2.2	08.80	18.92	18883	0538	07.36	0.10
161658.43+070355.42	1731-53884-442	2.0	2.5	07.17	19.45	09415	0135	08.04	0.20
155651.96+351218.94	1417-53141-512	2.0	1.5	08.59	19.54	07582	0091	08.04	0.19
101529.62+090703.83	1237-52762-533	2.0	K	12.24	18.60	06903	0049	10.00	0.01
153742.29+434719.76	1052-52466-619	2.0	-	04.11	20.07	37196	2306	07.67	0.36
145602.53-005548.75	0921-52380-528	2.0	2.0	04.72	19.56	14462	1133	08.08	0.21
133420.98+041751.09	0853-52374-198	2.0	2.6	12.65	18.53	17415	0493	09.24	0.06
155857.29+480047.44	0813-52354-328	2.0	2.6	07.83	19.28	14685	0556	09.02	0.12
112022.02+635437.54	0597-52059-308	2.0	1.9	05.19	19.27	07561	0098	08.02	0.33
144649.26+005215.44	0537-52027-126	2.0	2.2	04.78	19.94	13088	1128	08.33	0.23
022523.68+002743.09	0406-51900-543	2.0	1.7	05.47	20.01	11661	1025	08.20	0.29
171556.29+600643.89	0354-51792-318	2.0	K	05.87	19.34	12153	0797	08.46	0.29
113213.00-003036.88	0282-51658-278	2.0	2.2	07.44	19.82	14286	0636	07.68	0.21
152855.62-015148.79	0925-52411-312	1.8	-	05.25	20.08	21856	1156	07.64	0.23
160904.12+175337.90	2967-54584-089	1.8	1.9	08.61	19.20	14379	0431	07.71	0.10
084541.13+312936.60	2960-54561-009	1.8	2.0	05.33	20.67	11390	0283	08.93	0.22
121033.24+221402.64	2644-54210-167	1.8	1.9	34.91	17.07	15144	0096	08.56	0.02

Name (SDSS J)	P-M-F	$B_{H\alpha}$ (MG)	$B_{H\beta}$ (MG)	S/N	g (mag)	$T_{\text{eff}}$ (K)	$\sigma_T$ (K)	$\log g$ (cgs)	$\sigma_g$ (cgs)
131426.38+173228.14	2604-54484-481	1.8	1.9	14.77	18.62	07038	0054	09.95	0.06
103648.67+171045.20	2593-54175-131	1.8	2.6	06.22	19.63	13884	1289	07.97	0.26
092108.83+130111.65	2577-54086-448	1.8	2.1	07.20	19.65	13263	0538	07.84	0.13
110911.12+582209.38	2414-54526-301	1.8	2.6	06.74	20.30	19207	0681	07.66	0.13
100828.98+183633.49	2373-53768-290	1.8	2.0	04.74	20.15	09295	0177	08.74	0.23
091310.44+230042.60	2287-53705-541	1.8	2.2	06.42	20.03	17629	0586	08.22	0.12
081748.55+154341.15	2272-53713-386	1.8	1.2	07.35	19.49	17936	0460	08.21	0.11
080703.25+135537.87	2268-53682-472	1.8	1.7	06.79	19.88	12887	0494	08.26	0.14
163400.35+145651.38	2209-53907-472	1.8	2.2	03.64	20.39	13797	0820	08.06	0.22
040054.82-064625.27	2071-53741-014	1.8	1.8	08.56	19.64	18869	0721	07.28	0.13
004148.06-005127.47	1905-53706-253	1.8	2.6	07.63	20.08	13253	0551	08.07	0.13
	0691-52199-300	3.3	3.9	04.61					
233708.97+492532.00	1889-53240-584	1.8	2.2	09.97	19.58	09859	0100	08.23	0.12
123527.09+145318.64	1768-53442-074	1.8	2.2	06.55	19.55	15250	0466	07.78	0.11
232937.55+524437.90	1663-52973-119	1.8	1.8	14.00	18.95	32204	0370	08.22	0.08
080150.50+205012.05	1583-52941-599	1.8	-	03.51	20.43	11831	1244	08.32	0.35
214539.84+000136.44	0990-52465-080	1.8	-	07.16	19.55	30307	0802	07.92	0.18
010654.65-104315.01	0659-52199-207	1.8	1.7	09.57	19.19	08573	0102	07.70	0.22
094103.85+032835.84	0570-52266-279	1.8	2.2	04.69	20.07	19333	0964	07.88	0.27
113431.97-031528.99	0327-52294-131	1.8	1.7	07.09	19.57	16750	0584	09.12	0.10
144114.21+003702.40	0307-51663-595	1.8	1.8	06.57	19.87	16750	0507	08.07	0.11
075036.55+222021.48	2916-54507-133	1.7	1.7	08.18	20.29	18254	0555	07.82	0.11
035010.32+085829.18	2697-54389-048	1.7	1.7	06.47	20.32	11462	0558	07.81	0.23
071814.18+305148.75	2695-54409-268	1.7	1.7	05.88	20.47	12248	0839	08.12	0.21
064607.86+280510.14	2694-54199-175	1.7	2.1	20.67	18.69	22775	0288	09.05	0.04
172623.14+632607.81	2561-54597-212	1.7	1.6	07.16	20.42	18182	0643	08.07	0.13
163013.93+123941.95	2533-54585-325	1.7	2.2	07.17	19.86	12124	0289	08.11	0.13
160532.19+131748.69	2525-54569-425	1.7	1.9	04.00	20.28	12402	0549	07.65	0.22
154424.84+132650.84	2517-54567-110	1.7	1.7	11.80	18.97	13793	0736	07.93	0.09
030158.92+372204.26	2443-54082-190	1.7	-	12.67	19.57	28949	0432	08.06	0.09
084522.95+150020.36	2429-53799-152	1.7	2.3	08.36	19.35	17904	0432	07.79	0.10
084039.37+125706.28	2428-53801-354	1.7	1.7	05.39	19.63	10604	0232	07.97	0.20
082447.49+131543.26	2422-54096-588	1.7	1.8	05.91	19.45	19134	0545	07.81	0.14
104851.94+273817.72	2358-53797-156	1.7	1.9	07.33	19.20	10923	0175	07.75	0.14
021338.52+053023.40	2321-53711-125	1.7	2.2	06.27	20.20	09058	0132	08.14	0.23
053400.84+625419.80	2302-53709-579	1.7	2.1	05.24	20.81	10954	0569	08.11	0.23
091002.83+232220.03	2287-53705-470	1.7	1.7	06.17	19.94	15291	0538	07.76	0.12
084845.66+214047.05	2280-53680-446	1.7	1.7	07.74	19.73	19142	0502	07.86	0.10
224602.82+230704.18	2261-53612-559	1.7	1.8	10.63	19.56	17160	0327	08.07	0.07
113500.53+291206.62	2220-53795-222	1.7	-	06.31	19.65	21456	0667	07.79	0.14
161321.41+155332.09	2198-53918-400	1.7	1.7	05.01	19.92	09959	0189	07.98	0.25
174755.72+251232.33	2194-53904-154	1.7	-	09.34	19.75	10390	0122	08.32	0.14
074327.09+273732.37	2075-53730-278	1.7	1.5	11.21	19.88	08727	0101	07.07	0.36
074047.65+180907.32	2074-53437-237	1.7	-	14.31	19.27	17904	0299	07.94	0.06
073135.37+353108.57	2073-53728-108	1.7	1.5	05.30	20.36	22795	1052	07.85	0.17
052831.03+005244.22	2072-53430-336	1.7	1.5	14.13	19.52	16444	0300	08.03	0.06
053016.83-001034.50	2072-53430-233	1.7	1.7	05.79	20.44	16128	0888	07.87	0.17
084253.04+092226.54	1759-53081-618	1.7	2.1	09.14	19.15	11316	0955	07.91	0.17
083002.71+083632.04	1758-53084-531	1.7	1.6	08.21	19.42	15642	0388	07.81	0.09
134758.89+495427.49	1669-53433-020	1.7	1.9	19.25	17.79	16628	0181	08.56	0.04
144541.72+411441.59	1397-53119-352	1.7	1.0	06.06	19.94	24938	0802	07.25	0.20
014938.34-004938.03	0699-52202-012	1.7	2.6	07.23	19.35	16010	0488	07.89	0.11
082159.66+431127.28	0547-52207-019	1.7	-	05.36	20.15	09646	0901	05.12	0.13
162304.11+183522.23	2969-54586-617	1.5	1.6	10.64	19.16	14169	0665	08.08	0.08
075704.00+085520.06	2945-54505-148	1.5	1.2	09.92	20.01	18123	0424	07.95	0.09
044512.39-052524.52	2942-54521-487	1.5	-	06.52	20.44	12488	0430	08.62	0.15
192553.60+620708.70	2563-54653-165	1.5	1.7	06.54	19.94	10504	0177	09.04	0.18
030550.35+370759.16	2443-54082-154	1.5	-	10.04	19.79	12414	0483	07.93	0.13
084111.34+154921.03	2429-53799-358	1.5	1.3	06.67	19.79	18090	0487	07.91	0.12
004011.49+070255.73	2327-53710-074	1.5	1.7	12.11	19.52	18529	0381	08.09	0.07
212143.08-060005.77	2320-54653-445	1.5	-	12.02	19.74	25075	0624	08.02	0.08

Name (SDSS J)	P-M-F	$B_{H\alpha}$ (MG)	$B_{H\beta}$ (MG)	S/N	g (mag)	$T_{\text{eff}}$ (K)	$\sigma_T$ (K)	$\log g$ (cgs)	$\sigma_g$ (cgs)
083020.36+185814.55	2275-53709-229	1.5	-	12.78	19.02	22490	0432	08.69	0.07
203332.94+140115.37	2258-54328-295	1.5	1.3	11.02	20.22	18529	0436	07.78	0.08
235107.48+403454.05	1883-53271-521	1.5	2.2	07.67	20.14	16535	0505	08.92	0.10
080719.89+064536.58	1756-53080-234	1.5	1.5	04.49	20.16	12380	0912	07.92	0.29
162115.35+075059.05	1732-53501-455	1.5	1.7	06.72	19.83	16750	0501	07.75	0.12
141808.13+481850.59	1672-53460-181	1.5	2.6	08.95	19.10	14310	0313	06.99	0.10
203016.13+765022.67	1661-53240-116	1.5	2.0	05.11	20.31	13277	1567	07.72	0.26
143218.26+430126.72	1396-53112-338	1.5	-	09.83	19.00	25429	0590	07.94	0.10
112328.49+095619.39	1222-52763-625	1.5	1.7	18.25	17.74	10537	0057	08.70	0.06
160929.97+443857.20	0814-52370-317	1.5	1.7	05.40	19.75	40320	2355	08.17	0.32
145029.51+032218.84	0587-52026-016	1.5	-	09.45	19.12	14261	0444	07.85	0.09
095603.30+540907.05	0769-54530-078	1.4	1.7	07.88	19.51	12180	0456	07.58	0.17
154120.14+022756.54	0594-52045-315	1.4	1.7	05.33	20.05	19937	0923	07.66	0.21
065133.34+284423.44	2694-54199-528	1.3	1.6	18.18	19.11	17841	0265	07.06	0.05
122238.87+005034.42	2568-54153-411	1.3	1.7	11.39	19.87	12956	0470	07.86	0.09
163630.30+114452.39	2533-54585-502	1.3	1.6	05.77	20.30	10582	0215	08.48	0.20
093813.84+615600.92	2403-53795-278	1.3	1.6	08.63	20.14	14004	0475	07.80	0.10
101642.27+281610.22	2348-53757-040	1.3	1.7	05.46	19.81	24231	0897	07.80	0.17
212232.58-061839.74	2320-54653-537	1.3	0	17.06	19.38	26168	0557	07.70	0.07
130535.77+283014.60	2242-54153-447	1.3	-	09.68	19.36	28932	0465	07.90	0.10
082107.35+194433.68	2082-53358-617	1.3	-	08.84	19.13	25636	0795	07.44	0.11
004038.90+243852.77	2058-53349-195	1.3	-	12.05	19.72	14375	0385	07.79	0.08
105152.19+321135.19	2026-53711-183	1.3	2.0	05.74	20.01	14529	0741	09.08	0.16
123449.89+150348.87	1768-53442-557	1.3	-	13.20	18.81	06302	0007	10.00	0.01
155932.58+081904.62	1728-53228-175	1.3	1.0	04.81	20.22	10080	0206	08.26	0.28
133007.57+104830.59	1699-53148-137	1.3	2.0	11.52	18.90	07094	0065	08.56	0.13
170657.90+232118.99	1687-53260-019	1.3	1.7	07.79	19.24	22242	0648	08.07	0.10
201822.90+754807.62	1661-53240-124	1.3	2.5	05.10	20.32	14694	3140	07.94	0.24
203828.49+764123.07	1661-53240-023	1.3	2.0	06.03	19.90	11138	1504	08.82	0.27
161118.60+242446.65	1657-53520-372	1.3	1.5	09.93	19.13	08935	0082	07.85	0.13
142118.18+523547.17	1326-52764-250	1.3	1.5	04.57	19.71	21752	0836	08.47	0.17
083745.13+064313.82	1297-52963-637	1.3	-	07.41	19.74	25966	0829	07.91	0.12
093411.36+364641.28	1275-52996-174	1.3	2.0	06.56	19.68	13930	0604	09.03	0.14
084628.05+064532.83	1189-52668-344	1.3	2.0	04.23	20.05	17143	0781	08.27	0.24
161030.50+365442.22	1056-52764-440	1.3	2.0	08.94	19.24	19734	0448	09.28	0.08
100932.74+524638.21	0903-52400-584	1.3	2.0	16.11	18.60	15122	0295	09.09	0.05
093508.57+042116.76	0569-52264-452	1.3	-	06.90	19.86	11468	0697	08.17	0.20
092932.56+561318.58	0556-51991-326	1.3	2.0	07.93	19.61	08935	0093	07.77	0.18
121557.43+665344.84	0493-51957-104	1.3	-	09.78	19.14	06935	0087	09.18	0.29
031630.64-081529.03	0459-51924-002	1.3	1.6	11.01	19.05	11677	0203	09.09	0.11
075916.54+433519.06	0436-51883-045	1.3	2.1	11.63	18.74	22420	0459	09.62	0.08
012641.92+132537.21	0425-51844-283	1.3	-	11.40	18.60	08566	0052	05.04	0.05
022623.81-002313.09	0406-52238-071	1.3	1.7	05.13	19.80	08727	0134	05.07	0.08
022335.16+004954.90	0406-51900-490	1.3	-	07.16	19.77	07501	0097	07.69	0.21
220514.08-005841.67	0373-51788-243	1.3	-	11.87	18.69	32204	0473	07.83	0.11
121706.47+172856.02	2596-54207-023	1.2	-	07.07	19.16	23729	0838	08.09	0.14
083051.08+244615.73	2330-53738-503	1.2	2.2	10.85	19.78	16454	0355	08.02	0.07
013742.54+235138.27	2064-53341-491	1.2	1.7	07.14	20.24	14043	4018	08.37	0.39
233039.04+500729.68	1889-53240-377	1.2	-	09.86	19.53	10811	0139	08.29	0.10
082239.43+082436.75	1758-53084-346	1.2	-	18.83	18.12	11193	0077	08.56	0.05
165354.58+251738.46	1692-53473-213	1.2	1.0	03.78	20.35	12556	1473	07.88	0.30
172705.00+084857.15	2818-54616-374	1.0	-	28.38	18.42	41618	0550	08.02	0.06
140444.22+201922.62	2771-54527-196	1.0	1.3	10.31	19.15	13472	0367	08.12	0.08
093431.11+132814.70	2580-54092-273	1.0	-	10.85	19.02	34332	0631	08.07	0.12
084233.37+101806.35	2573-54061-141	1.0	-	11.20	19.06	12284	0225	08.40	0.09
155232.77+264636.67	2474-54564-392	1.0	-	11.18	19.89	19362	0409	07.89	0.08
124508.48+591551.78	2461-54570-264	1.0	-	07.93	19.94	17184	0475	08.04	0.10
133836.07+652433.09	2460-54616-042	1.0	-	09.55	19.73	22733	0667	07.93	0.10
024241.67+291608.32	2444-54082-604	1.0	1.1	12.63	19.44	29405	0429	07.80	0.08

Name (SDSS J)	P-M-F	$B_{H\alpha}$ (MG)	$B_{H\beta}$ (MG)	S/N	g (mag)	$T_{\text{eff}}$ (K)	$\sigma_T$ (K)	$\log g$ (cgs)	$\sigma_g$ (cgs)
103403.99+305034.45	2354-53799-536	1.0	-	06.38	19.51	14876	0430	07.89	0.11
212514.19-062152.52	2320-54653-612	1.0	-	07.72	20.25	11242	0246	08.39	0.15
211744.75-073652.87	2320-54653-312	1.0	-	12.54	19.53	32642	0486	09.51	0.10
093654.95+262650.24	2294-54524-617	1.0	1.6	08.25	19.61	15691	0401	07.92	0.09
091326.64+211250.50	2288-53699-332	1.0	-	09.65	18.82	14512	0430	08.14	0.08
131702.34+281848.62	2243-53794-533	1.0	-	10.90	19.08	11481	0175	08.32	0.09
172735.81+280536.92	2193-53888-570	1.0	-	14.64	19.37	18084	0292	07.91	0.06
154605.41+243759.05	1850-53786-312	1.0	-	08.82	18.78	06438	0067	09.29	0.13
140822.00+443007.96	1467-53115-557	1.0	-	10.49	19.02	15859	0279	07.21	0.08
160246.46+303914.48	1405-52826-283	1.0	-	37.79	16.06	60359	1229	07.32	0.07
060442.49+641357.12	2301-53712-476	$\leq 1$	-	19.01	19.09	67833	3013	10.00	0.00
132926.05+254936.50	2245-54208-307	$\leq 1$	-	23.52	17.42	28299	0175	09.39	0.04
080527.56+073534.16	2056-53463-557	$\leq 1$	-	24.66	17.89	06300	0003	10.00	0.01
165538.93+253345.99	1692-53473-163	$\leq 1$	-	29.73	16.94	11141	0052	09.38	0.03
081018.73+370010.95	0892-52378-374	$\leq 1$	-	21.31	18.14	09556	0042	08.37	0.05
143632.86+563525.43	0791-52435-304	$\leq 1$	-	07.50	18.70	06865	0079	09.85	0.14
075842.68+365731.59	0757-52238-439	$\leq 1$	-	14.61	19.01	06760	0048	08.15	0.11
162727.70+492507.99	0625-52145-578	$\leq 1$	-	10.33	18.98	08449	0079	09.96	0.06
145636.33+583321.24	0610-52056-189	$\leq 1$	-	06.30	19.64	07601	0100	07.85	0.30
100732.64+010914.60	0501-52235-004	$\leq 1$	-	07.29	19.58	07215	0101	07.39	0.27
085309.10+563441.51	0483-51924-203	$\leq 1$	-	07.92	19.62	07889	0101	07.77	0.22
173235.20+590533.46	0366-52017-591	$\leq 1$	-	12.92	18.73	10818	0098	08.03	0.09

**Table 1.** Magnetic White Dwarf Stars. Notes: P-M-F are the Plate-Modified Julian Date-Fiber number that designates an SDSS spectrum. K in the  $H\beta$  magnetic field column means it was measured by Külebi et al. (2009). For those spectra we quote only their field determinations, as they fit the whole spectrum, keeping  $\log g = 8.0$ . \*SDSS J125044.42+154957.3 is a  $P_{\text{orb}} = 86$ m binary (Breedt et al. 2012).